INCORPORATING RIGOROUS HEIGHT DETERMINATION INTO UNIFIED FRACTURE DESIGN

A Thesis

by

TERMPAN PITAKBUNKATE

Submitted to the Office of Graduate Studies of
Texas A&M University
in partial fulfillment of the requirements for the degree of

MASTER OF SCIENCE

August 2010

Major Subject: Petroleum Engineering

Incorporating Rigorous Height Determination into Unified Fracture Design

INCORPORATING RIGOROUS HEIGHT DETERMINATION INTO UNIFIED FRACTURE DESIGN

A Thesis

by

TERMPAN PITAKBUNKATE

Submitted to the Office of Graduate Studies of
Texas A&M University
in partial fulfillment of the requirements for the degree of

MASTER OF SCIENCE

Approved by:

Chair of Committee,	Peter P. Valko
Committee Members,	Christine Ehlig-Economides
	Steven Taliaferro
Head of Department,	Stephen A. Holditch

August 2010

Major Subject: Petroleum Engineering

ABSTRACT

Incorporating Rigorous Height Determination into

Unified Fracture Design. (August 2010)

Termpan Pitakbunkate, B.Eng., Chulalongkorn University

Chair of Advisory Committee: Dr. Peter P. Valko

Hydraulic fracturing plays an important role in increasing production rate in tight reservoirs. The performance of the reservoir after fracturing can be observed from the productivity index. This parameter is dependent on the fracture geometry; height, length and width.

Unified fracture design (UFD) offers a method to determine the fracture dimensions providing the maximum productivity index for a specific proppant amount. Then, in order to achieve the maximum productivity index, the treatment schedules including the amount of liquid and proppant used for each stage must be determined according to the fracture dimensions obtained from the UFD.

The proppant number is necessary for determining the fracture geometry using the UFD. This number is used to find the maximum productivity index for a given proppant amount. Then, the dimensionless fracture conductivity index corresponding to the maximum productivity index can be computed. The penetration ration, the fracture length, and the propped fracture width can be computed from the dimensionless fracture conductivity. However, calculating the proppant number used in UFD requires the

fracture height as an input. The most convenient way to estimate fracture height to input to the UFD is to assume that the fracture height is restricted by stress contrast between the pay zone and over and under-lying layers. In other words, the fracture height is assumed to be constant, independent of net pressure and equal to the thickness of the layer which has the least minimum principal stress. However, in reality, the fracture may grow out from the target formation and the height of fracture is dependent on the net pressure during the treatment. Therefore, it is necessary to couple determination of the fracture height with determination of the other fracture parameters.

In this research, equilibrium height theory is applied to rigorously determine the height of fracture. Solving the problem iteratively, it is possible to incorporate the rigorous fracture height determination into the unified fracture design.

DEDICATION

I would like to dedicate this work to my parents, brother and sisters for their encouragement and love.

ACKNOWLEDGEMENTS

I would like to take this opportunity to thank my committee chair, Dr. Peter Valko, for very good advices and help on my research. He always pointed out the right path for my work. He also inspired me to pursue the next level of education.

I also would like to thank my committee members, Dr. Christine Economides and Dr. Steven Taliaferro, for their guidance and support throughout the course of this research.

I also appreciate the help from my colleagues and the department faculty and staff. They offered their support, knowledge and work experience which were so helpful to my research.

Thanks also go to all of my friends at Texas A&M University for making my time a great and invaluable experience.

Finally, I would like to acknowledge the financial support from Schlumberger. The facilities and resources provided by the Harold Vance Department of Petroleum Engineering at Texas A&M University are gratefully acknowledged.

NOMENCLATURE

Symbol		Description
a	=	fracture half-height, L, ft
asp	=	fracture aspect ratio
A	=	reservoir drainage area, L^2, acre
A_f	=	fracture surface area, L^2, ft^2
c	=	proppant concentration, m/L^3, ppg
c_e	=	proppant concentration at the end of the job, m/L^3, ppg
c_{added}	=	added proppant concentration, m/L^3, ppga
C_{fD}	=	dimensionless fracture conductivity
C_L	=	leak-off coefficient, $L/t^{0.5}$, $ft/min^{0.5}$
E	=	Young's modulus, m/Lt^2, psi
E'	=	plane strain modulus, m/Lt^2, psi
h_f	=	fracture height, L, ft
h_n	=	thickness of net pay, L, ft
h_p	=	thickness of perforation interval, L, ft
Δh_d	=	fracture growth into lower bounding formation, L, ft
Δh_u	=	fracture growth into upper bounding formation, L, ft
I_x	=	penetration ratio

J	=	well productivity index, L^4t^2/m, bbl/psi
J_D	=	well dimensionless productivity index
k	=	reservoir permeability, L^2, md
k_{00}	=	pressure at center of crack, m/Lt^2, psi
k_1	=	hydrostatic gradient, m/ L^2t^2, psi/ft
k_f	=	propped fracture permeability, L^2, md
K	=	rheology consistency index, m/Lt^2, lbf/ ft^2
K_I	=	stress intensity for opening crack, $m/L^{0.5}t^2$, $psi\text{-}in^{0.5}$
$K_{I,bottom}$	=	stress intensity at bottom tip of crack, $m/L^{0.5}t^2$, $psi\text{-}in^{0.5}$
$K_{I,top}$	=	stress intensity at top tip of crack, $m/L^{0.5}t^2$, $psi\text{-}in^{0.5}$
K_{IC}	=	fracture toughness, $m/L^{0.5}t^2$, $psi\text{-}in^{0.5}$
K_{IC2}	=	fracture toughness of upper layer, $m/L^{0.5}t^2$, $psi\text{-}in^{0.5}$
K_{IC3}	=	fracture toughness of lower layer, $m/L^{0.5}t^2$, $psi\text{-}in^{0.5}$
K'	=	modulus of cohesion, $m/L^{0.5}t^2$, $psi\text{-}in^{0.5}$
M_{prop}	=	proppant mass, m, lbm
$M_{prop,stage}$	=	proppant mass required for each stage, m, lbm
n	=	rheology flow behavior index
N_{prop}	=	proppant number
Δp	=	pressure difference, m/Lt^2, psi

p_b	=	breakdown pressure or rupture pressure, m/Lt^2, psi
p_c	=	fracture closure pressure, m/Lt^2, psi
p_{cp}	=	pressure at center of perforation, m/Lt^2, ps
p_r	=	fracture reopening pressure, m/Lt^2, psi
p_{net}	=	net pressure at center of perforation, m/Lt^2, psi
p_{nw}	=	net pressure at center of crack, m/Lt^2, psi
$p_n(x)$	=	net pressure at any location in x-direction, m/Lt^2, psi
$p_n(y)$	=	net pressure at any location in y-direction, m/Lt^2, psi
q_i	=	slurry injection rate for one-wing, L^3/t, bbl/min
q_p	=	production rate, L^3/t, bbl/min
r_e	=	reservoir drainage radius, L, ft
S_f	=	fracture stiffness, m/ L^{2}t^2, psi/in
S_p	=	spurt loss coefficient, L, ft
t_e	=	pumping time, t, min
t_{paD}	=	padding time, t, min
T_0	=	tensile strength, m/Lt^2, psi
u_{avg}	=	average velocity of slurry in fracture, L/t, ft/s
V_f	=	fracture volume, L^3, ft^3
V_i	=	total slurry injection volume, L^3, ft^3

V_{paD}	=	padding volume, L^3, gal
V_{prop}	=	proppant volume, L^3, ft^3
V_{res}	=	reservoir volume, L^3, ft^3
V_{stage}	=	liquid volume required for each stage, L^3, gal
w	=	propped fracture width, L, in
$\overline{w}$	=	average hydraulic fracture width, L, in
$w_0(x)$	=	max. hydraulic fracture width at any location, L, in
$w_{w,0}$	=	max. hydraulic fracture width at wellbore, L, in
W	=	work to extend a crack, mL^2/t^2, psi-ft^3
x	=	distance from wellbore, L, ft
x_e	=	reservoir length, L, ft
x_f	=	fracture half-length, L, ft
y	=	dimensionless vertical position
y_d	=	dimensionless vertical position of bottom perforation
y_u	=	dimensionless vertical position of top perforation
y_m	=	distance from center of crack in y-direction, L, ft

Greek

γ	=	shape factor
γ_w	=	surface energy of fracture, mL/t^2, psi-ft^2
ε	=	exponent of the proppant concentration curve

$\in$	=	strain
κ	=	Nolte's function at $\Delta t = 0$
η	=	slurry efficiency
η_0	=	ratio of fracture volume in net pay to total fracture volume
ϕ_p	=	fracture packed porosity
ρ_p	=	proppant density, m/ L^3, lbm/ft^3
σ	=	normal stress, m/Lt^2, psi
$\sigma(y)$	=	normal stress at any location in y-direction, m/Lt^2, psi
σ_h	=	minimum horizontal in-situ stress, m/Lt^2, psi
σ_H	=	maximum horizontal in-situ stress, m/Lt^2, psi
$\Delta\sigma_{avg}$	=	average stress difference, m/Lt^2, psi
$\Delta\sigma_d$	=	stress diff. of reservoir and lower formation, m/Lt^2, psi
$\Delta\sigma_u$	=	stress diff. of reservoir and upper formation, m/Lt^2, psi
τ	=	shear stress, m/Lt^2, psi
μ	=	viscosity, m/Lt, cp
μ_e	=	equivalent Newtonian viscosity, m/Lt, cp
μ_f	=	friction coefficient, L, in
ν	=	Poisson's ratio

TABLE OF CONTENTS

CHAPTER Page

LIST OF FIGURES

FIGURE Page

FIGURE Page

LIST OF TABLES

TABLE Page

CHAPTER I

INTRODUCTION

In recent times, the energy problem has been getting more critical. In addition, it is known that petroleum which is the main energy resource is limited. Most of new reservoirs which have been discovered recently are unconventional such as tight gas reservoir. Meanwhile, the pressure of current producing reservoirs keeps declining. As a result, there is no energy enough to drive the fluid from the formation to the well. Petroleum engineers would provide completion designs or techniques to either produce hydrocarbon from those unconventional reservoirs or enhance productivity of the current producing reservoirs. Hydraulic fracturing (propped fracturing) is one of completion techniques to improve well performance, in particular, in low permeability formation.

For the well which has a large skin factor due to drilling fluid damage or is located in a formation of low permeability, a fracture (low resistant path) is created for the fluid to bypass the skin or low permeability media (high resistant path) to the well. As a result, less pressure difference is required for fluid flow from the reservoir to the well. In other words, well productivity index increases. After fracturing, flow regime changes from radial flow to linear flow (see **Fig. 1.1**). Therefore, wellbore radius is not a restriction anymore (change of the streamlines structure).

This thesis follows the style of *SPE Journal.*

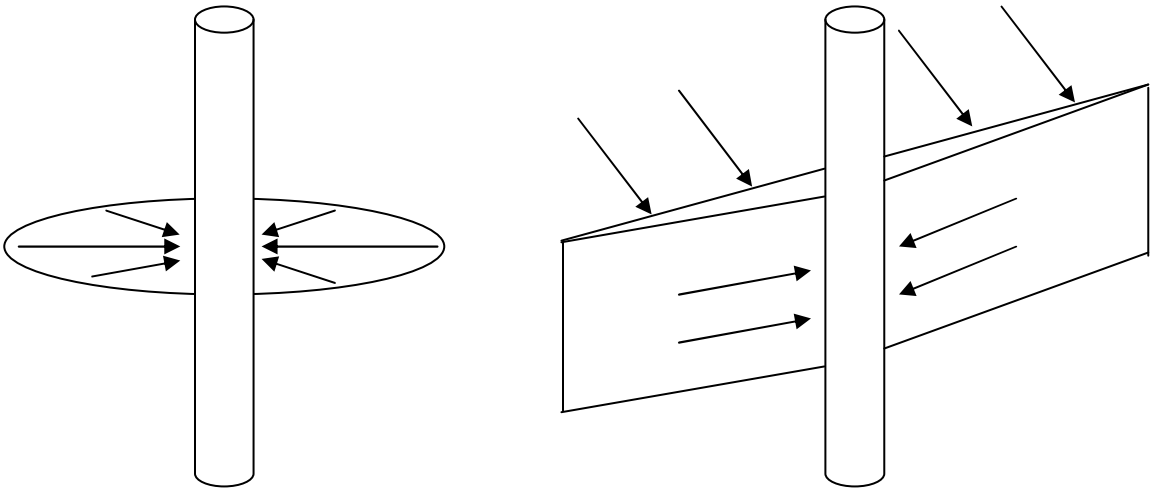

Fig. 1.1−Flow regime before (left) and after (right) hydraulic fracturing. Normally, radial flow occurs in case of an unfractured well but it will change to linear flow after fracturing

With hydraulic fracturing, the well production index is increasing. However, it is not insignificant, how much resources are used on the operation. The ultimate goal is to achieve the possible maximum improvement from a given amount of resources.

1.1 Literature Review

1.1.1 Fracture Propagation

To initiate a crack in the rock, it is necessary to introduce pressure to overcome breakdown pressure of the formation. Hubbert and Willis (1957) showed that whenever the stress field is anisotropic, fracture propagates in the plane perpendicular to minimum principle in-situ stress as shown in the **Fig. 1.2** because the fracture prefers to take the path of least resistance and therefore opens up against the smallest stress. Once the

fracture created, as long as the pressure is greater than the stress normal to the plane of the fracture which is equal to the closure pressure, p_c, it will continue to propagate.

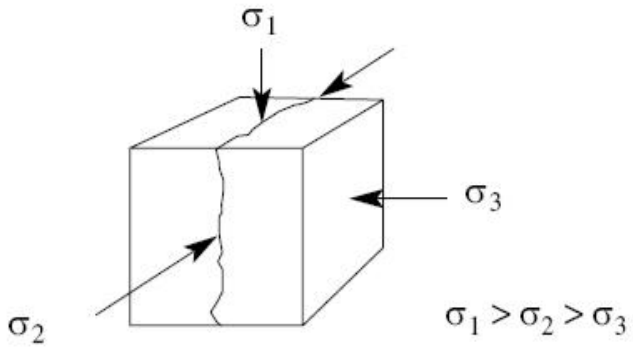

Fig. 1.2−Effect of in-situ stresses on fracture azimuth

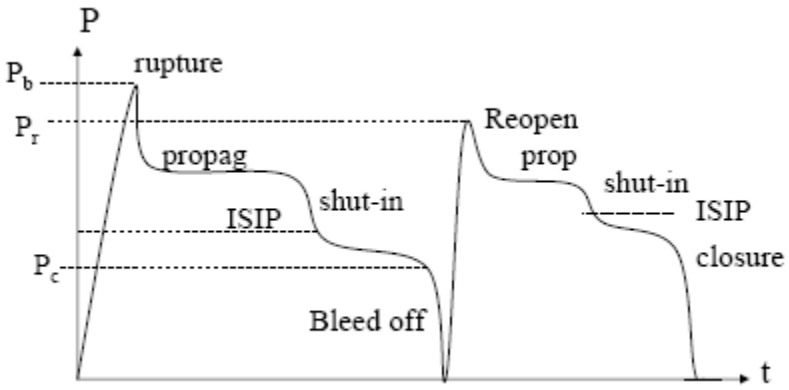

Fig. 1.3−Pressure profile of fracture propagation behavior

Fig. 1.3 shows the pressure profile of fracture propagation behavior which can be obtained from mini-frac job. The data from mini-frac analysis is interpreted to determine initial stresses; minimum in-situ stress, σ_h and maximum in-situ stress, σ_H. The fracture fluid is injected into the well and pressurized to create a fracture in the reservoir. To initiate the crack in the reservoir, the downhole pressure must overcome the

breakdown pressure (the peak of the first cycle). After the crack is created, the downhole pressure decreases and the fracture continues to propagate into the reservoir. The fracture closure pressure can be evaluated after stop injecting. The observation of the closure pressure is also shown in **Fig. 1.3**. The second cycle almost seems identical to the first one. However, it requires lower downhole pressure to reopen the fracture (reopening pressure, p_r) in the reservoir than it does for fracture creation ($p_b > p_r$).

Assuming that water doesn't penetrate into the formation, elastic solution can be used to determine the stress distribution around the borehole (σ_h and σ_H determination). The minimum in-situ stress is equal to closure pressure. The uniaxial tensile strength, T_0, can be determined from the difference of the breakdown pressure and reopening pressure. According to the condition of the vertical tensile crack as shown in **Fig. 1.4**, the stress at the wall of the borehole in the plane that perpendicular to the minimum in-situ stress (point A) should be equal to uniaxial tensile strength.

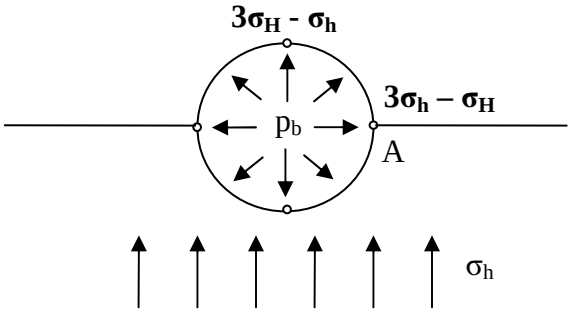

Fig. 1.4−The condition of the vertical tensile crack

Elastic solution equations

$$\sigma_h = p_c \quad \ldots\ldots\ldots\ldots\ldots\ldots\ldots\ldots\ldots\ldots\ldots\ldots\ldots\ldots\ldots\ldots\ldots\ldots \quad (1.1)$$

$$T_0 = p_b - p_r \quad \ldots\ldots\ldots\ldots\ldots\ldots\ldots\ldots\ldots\ldots\ldots\ldots\ldots\ldots\ldots\ldots\ldots\ldots \quad (1.2)$$

$$3\sigma_h - \sigma_H - p_b = T_0 \quad \ldots\ldots\ldots\ldots\ldots\ldots\ldots\ldots\ldots\ldots\ldots\ldots\ldots\ldots\ldots\ldots\ldots\ldots \quad (1.3)$$

The elastic solution equations are used to evaluate the formation (rock) strength. The minimum in-situ stress is used to calculate the fracture geometry. This information is necessary for the treatment schedule determination.

Moreover, the mini-frac is performed to determine the fracture toughness of the formation. The fracture toughness is the property which describes the ability of the rock to resist fracture. It is denoted by K_{IC} and has the unit of $Pa\sqrt{m}$ or $psi\sqrt{in}$. The higher fracture toughness is, the harder the crack will propagate in the rock. This parameter must be measured in not only the target formation but also the upper and lower bounding formations because these values are necessary for fracture height calculation using equilibrium height. It will be described in detail in the fracture height calculation section.

1.1.2 2D Fracture-Propagation Model

The fracture propagation models used in the engineering are derived by combination of elasticity, fluid flow, material balance and additional propagation criteria. With given injection fluid properties, injection rate and rock properties, a model will predict the changing in fracture dimensions and the wellbore pressure.

For the design purpose, the approximation of fracture geometry should be sufficient. In this research, the add-in fracture design program for treatment schedule determination is based on the fixed proppant mass and fracture height. With the given proppant mass and fracture height, fracture half-length can be determined using UFD methodology. After the fracture length is obtained, the simple fracture propagation models (2D fracture-propagation models) are used to predict the hydraulic fracture width at the end of pumping.

The models to simulate the propagation are based on the assumptions of plane strain. Therefore, two classes can be distinguished:

- Plane strain condition in horizontal plane and
- Plane strain condition in vertical plane.

If one considers an infinite elastic medium and that each horizontal section deforms independently from the others with no vertical strain, then it is called horizontal plane strain. All the z-components of the strain tensor vanish and in terms of strains:

$$\in_{xx} = \frac{1+\nu}{E}\left[(1-\nu)\sigma_{xx} - \nu\sigma_{yy}\right] \quad \ldots\ldots \quad (1.4)$$

$$\in_{yy} = \frac{1+\nu}{E}\left[(1-\nu)\sigma_{yy} - \nu\sigma_{xx}\right] \quad \ldots\ldots \quad (1.5)$$

$$\in_{xy} = \frac{1+\nu}{E}\tau_{xy} \quad \ldots\ldots \quad (1.6)$$

$$\in_{xz} = \in_{yz} = \in_{zz} = 0 \quad \ldots\ldots \quad (1.7)$$

For the horizontal plane strain geometry, the fracture zones should deform independently of the upper and lower layers. This would occur for free slippage on these

layers, or approximately represent a fracture with a horizontal penetration much smaller than the vertical one.

For the vertical plane strain, each vertical cross section deforms independently of the others. This case would approximate a fracture with a horizontal penetration much larger than the vertical penetration. Term of strains can be shown as followings.

$$\in_{zz} = \frac{1+\nu}{E}\left[(1-\nu)\sigma_{zz} - \nu\sigma_{yy}\right] \quad \text{(1.8)}$$

$$\in_{yy} = \frac{1+\nu}{E}\left[(1-\nu)\sigma_{yy} - \nu\sigma_{zz}\right] \quad \text{(1.9)}$$

$$\in_{yz} = \frac{1+\nu}{E}\tau_{yz} \quad \text{(1.10)}$$

$$\in_{xy} = \in_{xz} = \in_{xx} = 0 \quad \text{(1.11)}$$

Perkins-Kern width equation

Perkins and Kern (1961) assumed that a fixed height vertical fracture is propagated in well-confined zone. The PKN model assumes that the condition of plane strain holds in every vertical plane normal to the direction propagation which means that each vertical cross section deforms individually and is not affected by neighbors. In addition to the plane strain assumption, the fracture fluid pressure is assumed to be constant in vertical cross section which is perpendicular to the direction of propagation. The fracture cross section is elliptical with the maximum width at the center proportional to the net pressure at the point.

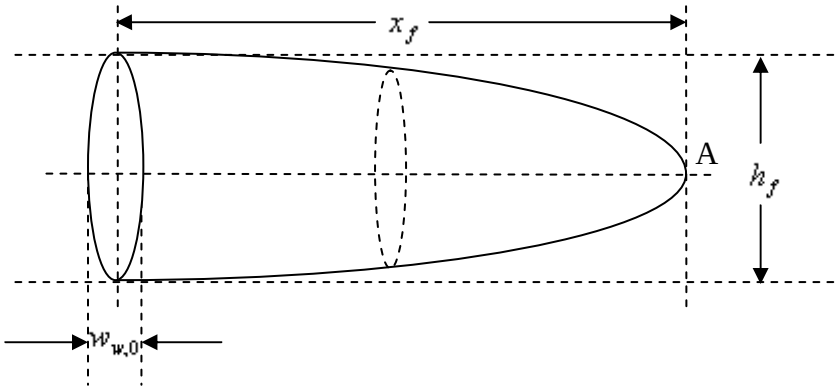

Fig. 1.5−Fracture propagation schematic according to the PKN model

The maximum width can be calculated using Eq. (1.12).

$$w_0 = \frac{2h_f p_n(x)}{E'} \quad \text{.....} \quad (1.12)$$

where E' is plane strain modulus which is evaluated by Eq. (1.13).

$$E' = \frac{E}{1-\nu^2} \quad \text{.....} \quad (1.13)$$

Perkins and Kern (1961) proposed that the net pressure at the tip of the fracture (point A in **Fig. 1.5**) is equal to zero, and the fluid pressure gradient in the propagating direction is determined by the flow resistance in a narrow, elliptical flow channel:

$$\frac{\partial p_n(x)}{\partial x} = -\frac{4\mu q_i}{\pi w_0^{\,3} h_f} \quad \text{.....} \quad (1.14)$$

Combining the Eq. (1.12) and (1.14) and integrating with the zero net pressure condition at the tip, the maximum fracture width profile at any location in the direction of propagation can be derived as shown in Eq. (1.15).

$$w_0(x) = w_{w,0}\left(1-\frac{x}{x_f}\right)^{1/4} \quad \text{.....} \quad (1.15)$$

where $w_{w,0}$ is the maximum hydraulic fracture width at the wellbore which is given (in term of petroleum industry) by

$$w_{w,0} = 3.27\left(\frac{\mu q_i x_f}{E'}\right)^{1/4} \quad \text{...} \quad (1.16)$$

The above equation is used to calculate the maximum width at the wellbore. In order to finding the average width of the fracture, the maximum width must be multiplied by the shape factor, γ, which contains two elements. The first one which is $\pi / 4$ is the factor to average the ellipse width in the vertical plane and the other one is the laterally averaged factor which is equal to $4/5$.

$$\overline{w} = \gamma w_{w,0} = \frac{\pi}{4}\frac{4}{5} w_{w,0} = \frac{\pi}{5} w_{w,0} \quad \text{...} \quad (1.17)$$

Assuming that q_i, x_f and E' are known, the only unknown in Eq. (1.16) for maximum fracture width calculation is μ. Using the formula for equivalent Newtonian viscosity of Power law fluid flowing in a limiting ellipsoid cross section:

$$\mu_e = K\left[\frac{1+(\pi-1)n}{\pi n}\right]^n \left(\frac{2\pi u_{avg}}{w_0}\right)^{n-1} \quad \text{...} \quad (1.18)$$

where u_{avg} is linear velocity:

$$u_{avg} = \frac{q_i}{h_f \overline{w}} \quad \text{..} \quad (1.19)$$

and combining the Eq. (1.16) to (1.19), the maximum fracture width at the wellbore can be solved as shown below.

$$w_{w,0} = 3.98^{\frac{n}{2+2n}} 9.15^{\frac{1}{2+2n}} K^{\frac{1}{2+2n}} \left(\frac{1-(\pi-1)n}{n} \right)^{\frac{n}{2+2n}} \left(\frac{h_f^{1-n} q_i^n x_f}{E'} \right)^{\frac{1}{2+2n}} \quad \text{....} \quad (1.20)$$

Khristianovich-Zheltov-Geertsma-deKlerk width equation

Kristianovich and Zheltov (1955) derived a solution for the propagation of a hydraulic fracture by that horizontal plane strain is held. As a result, the fracture width does not depend on the fracture height, except through the boundary condition at the wellbore. The fracture characteristics of KGD model is shown in **Fig. 1.6**. The fracture has rectangular cross section and its width is constant in the vertical plane because theory is based on the plane strain condition, which was applied to derive a mechanically satisfying model in individual horizontal plane. The fluid pressure gradient in the propagating direction is determined by the flow resistance in a narrow rectangular slit of variable width in the vertical direction. The KGD width equation is

$$w_{w,0} = 3.22 \left(\frac{\mu q_i x_f^{\,2}}{E' h_f} \right)^{1/4} \quad \text{……...} \quad (1.21)$$

The average fracture width of this model is (has no vertical component)

$$\overline{w} = \gamma w_{w,0} = \frac{\pi}{4} w_{w,0} \quad \text{…...……...} \quad (1.22)$$

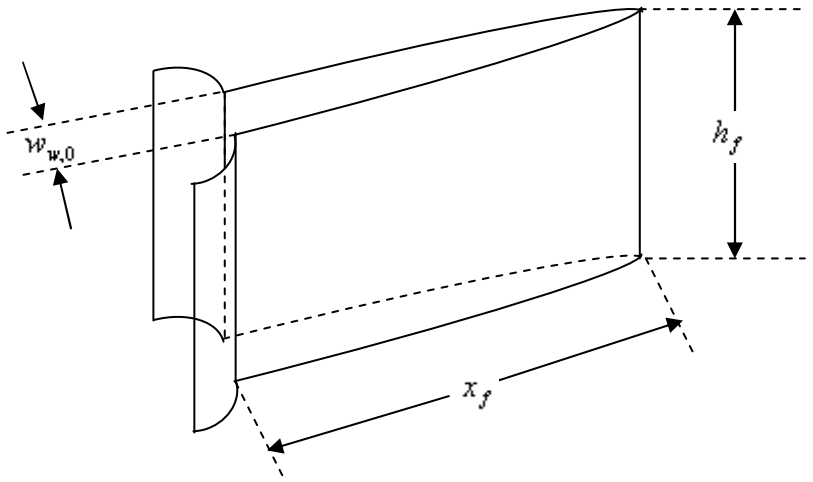

Fig. 1.6−Fracture propagation schematic according to the KGD model

The final equation to determine the maximum fracture width of KGD model is

$$w_{w,0} = 3.24^{\frac{n}{2+2n}} 11.1^{\frac{1}{2+2n}} K^{\frac{1}{2+2n}} \left(\frac{1+2n}{n}\right)^{\frac{n}{2+2n}} \left(\frac{q_i^n x_f^{\,2}}{E' h_f^n}\right)^{\frac{1}{2+2n}} \quad \text{..... (1.23)}$$

1.1.3 Unified Fracture Design

Economides et al. (2002) introduced the concept called Unified Fracture Design (UFD). It offers a method to determine the fracture dimensions providing the maximum reservoir performance after fracturing with the limited amount of proppant. In term of economics, to achieve the maximum reservoir performance means that to maximize the production rate. The parameter, which represents the production rate very well, is productivity index. The higher productivity index is, the more production gains. As a result, in the UFD, the dimensionless productivity, J_D, is observed.

$$J = \frac{q_p}{\Delta p} \quad \text{…….....} \quad (1.24)$$

The proppant number, N_{prop}, is an important parameter for the UFD. The proppant number is a dimensionless parameter and defined as

$$N_{prop} = I_x^2 C_{fD} \quad \text{…….....} \quad (1.25)$$

where I_x is a penetration ratio and

C_{fD} is a dimensionless fracture conductivity.

The penetration ratio is the ratio of the fracture length, $2x_f$, to the equivalent reservoir length, x_e. The dimensionless fracture conductivity is the ratio of the flow potential from the fracture to the well to that from the reservoir to the fracture as shown in eq. (1.26). The correlation of the equivalent reservoir length and the reservoir radius is shown in the Eq. (1.28) and **Fig. 1.7.**

$$I_x = \frac{2x_f}{x_e} \quad \text{……} \quad (1.26)$$

$$C_{fd} = \frac{k_f w}{k x_f} \quad \text{…….……} \quad (1.27)$$

$$A = r_e^2 \pi = x_e^2 \quad \text{……...……} \quad (1.28)$$

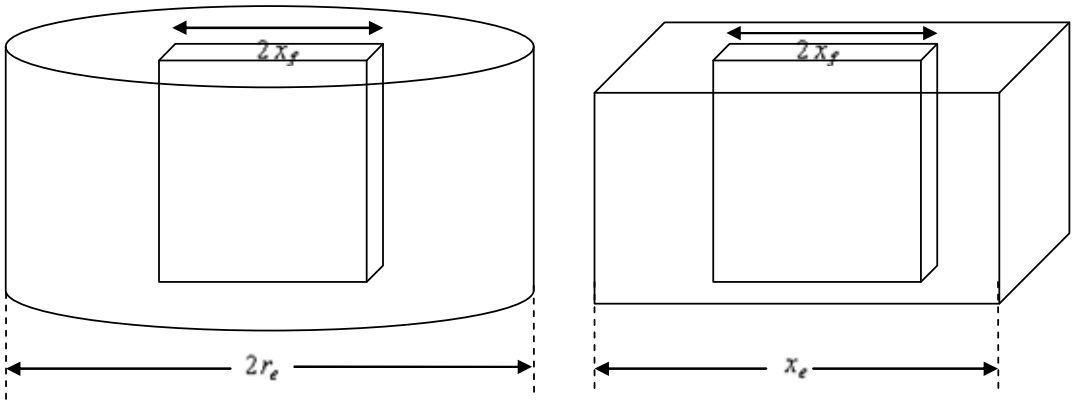

Fig. 1.7−Notation for fracture performance

Substituting Eq. (1.26) and (1.27) into Eq. (1.25), the correlation to determine the proppant number can be written as

$$N_{prop} = \frac{4k_f x_f w}{kx_e^{\,2}} = \frac{2k_f}{k}\frac{2x_f wh_n}{x_e^{\,2}h_n} = \frac{2k_f}{k}\frac{V_{prop}}{V_{res}} \quad \text{……..…..... (1.29)}$$

where V_{prop} is the volume of the propped fracture in the net pay. This number can be determined from the mass of proppants for the fracturing operation. However, the proppants do not only go in net pay but also fill the whole fracture. In order to use the mass of proppants to estimate V_{prop}, it requires to multiply with the ratio of the net height to the fracture height.

$$V_{prop} = \frac{M_{prop}\eta_0}{(1-\phi_p)\rho_p} \approx \frac{M_{prop}\left(\frac{h_n}{h_f}\right)}{(1-\phi_p)\rho_p} \quad \text{……. (1.30)}$$

From the calculated proppant number, the maximum dimensionless productivity index can be computed using the correlation as shown in **Fig 1.8 and 1.9**. From the plot, the dimensionless fracture conductivity corresponding to the maximum productivity index can be determined. Then, the penetration ratio, the fracture half-length and the propped fracture width can be calculated using Eq. (1.25), Eq. (1.26) and Eq. (1.27). After obtaining the fracture dimensions, the treatment schedules must be determined based on this fracture geometry in order to achieve the maximum productivity index.

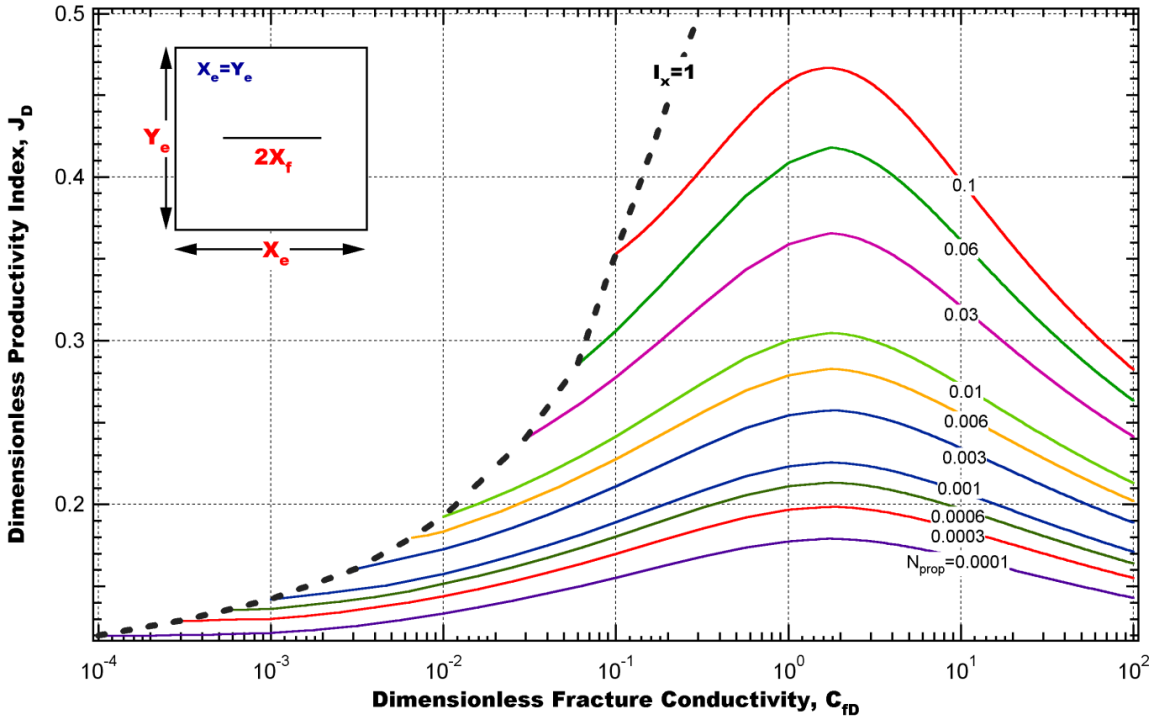

Fig. 1.8−Dimensionless productivity index as a function of dimensionless fracture conductivity for $N_{prop} < 0.1$ **[Unified Fracture Design, P.29]**

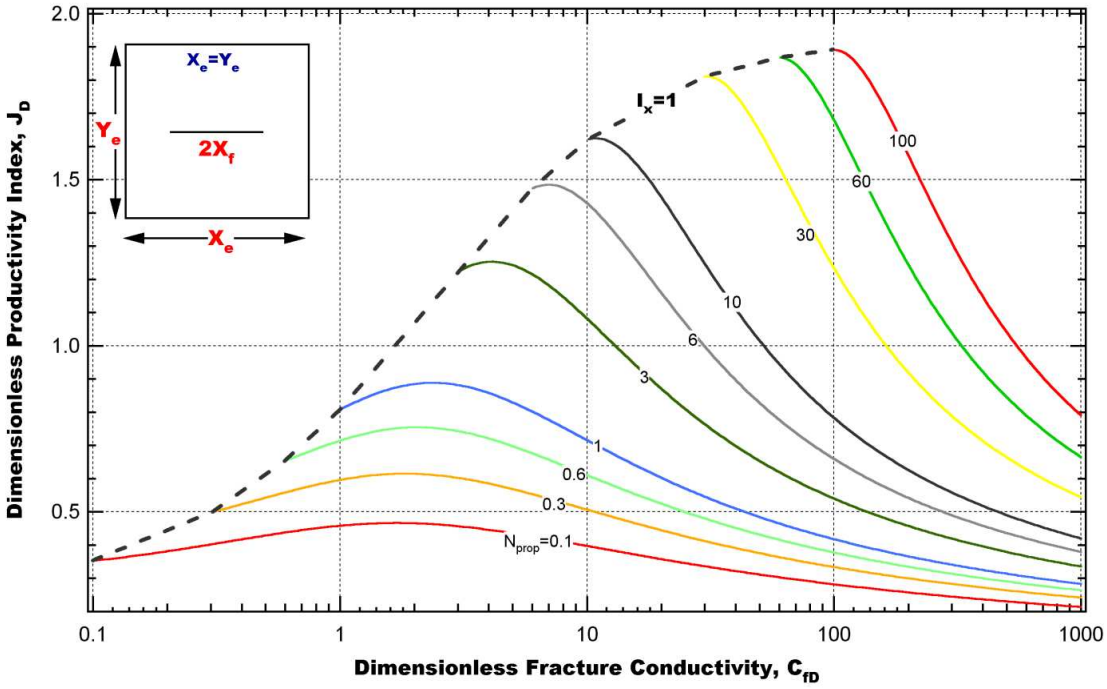

Fig. 1.9−Dimensionless productivity index as a function of dimensionless fracture conductivity for $N_{prop} > 0.1$ [Unified Fracture Design, P.30]

1.1.4 Treatment Schedule Determination

The purpose of hydraulic fracture design is to calculate the volume of fluid and proppants required to create a fracture with desired dimensions and conductivity.

Total injection time is one of important key factors of the fracture design. The total injection time starts from padding until finishing the whole proppants injection into the fracture. Material balance as shown as Eq. (1.31) is analyzed in order to determine the total injecting time.

Injecting Vol. = Fracture Vol. + Leak-off + Spurt Loss …….. (1.31)

$$V_i = V_f + 2A_f S_p + 2\kappa A_f C_L \sqrt{t_e} \quad \text{……..……..} \quad (1.32)$$

where κ is Nolte's function at $\Delta t = 0$ ($\kappa = g(0, \alpha)$). Eq. (1.32) can be rearranged as

$$\frac{q_i}{A_f} t_e - 2\kappa A_f C_L \sqrt{t_e} - 2S_p - \frac{V_f}{A_f} = 0 \quad \text{……..……..... (1.33)}$$

Solving Eq. (1.33), total injection time can be obtained.

According to Nolte (1986), the proppant schedule is derived from the requirement that

- The whole length created should be propped.
- The proppant distribution is uniform at the end of pumping.
- The proppant schedule should be the form of a delayed power law with the exponent, ε , and fraction of pad being equal.

The exponent of the proppant concentration curve (see **Fig. 1.10**) is derived from the fluid efficiency, η .

$$\varepsilon = \frac{1-\eta}{1+\eta} \quad \text{……..……..... (1.34)}$$

$$\eta = \frac{V_f}{V_i} = \frac{V_f}{q_i t_e} \quad \text{……...……..……..... (1.35)}$$

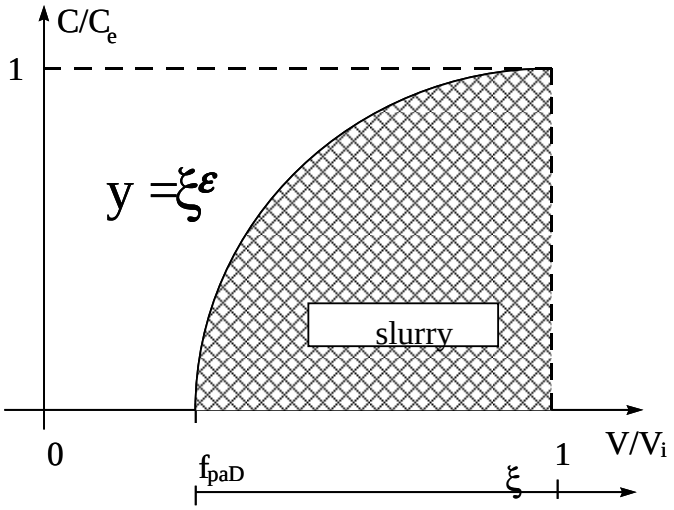

Fig. 1.10−Proppant concentration curve according Nolte (1986)

Padding volume, V_{paD} , and padding time, t_{paD} , (f_{paD} in **Fig. 1.10**) can be determined using the exponent of the proppant concentration curve obtained from Eq. (1.34).

$$t_{paD} = \varepsilon t_e \quad \text{.....} \quad (1.36)$$

$$V_{paD} = \varepsilon V_i \quad \text{.....} \quad (1.37)$$

As a requirement, all of injected proppants go inside the created fracture and the proppant distribution is uniform at the end of pumping. As a result, the proppant concentration at the end of the job can be derived from the mass of proppants divided by the volume of the fracture.

$$c_e = \frac{M_{prop}}{\eta V_i} \quad \text{.....} \quad (1.38)$$

Combining total injection time from Eq. (1.33), padding time from Eq. (1.36), and concentration at the end of the job from Eq. (1.38), the proppant concentration curve

or treatment schedule which is similar to **Fig. 1.10** can be generated using the following correlation;

$$c = c_e \left(\frac{t - t_{paD}}{t_e - t_{paD}} \right)^{\varepsilon} \quad \text{…….……..... (1.39)}$$

In order to calculate the mass of proppants and clean liquid required for each stage, it is more convenient if the proppant concentration is converted to mass of proppants added per unit volume of clean liquid using Eq. (1.40).

$$c_{added} = \frac{c}{1 - \frac{c}{\rho_p}} \quad \text{…….……..……..... (1.40)}$$

Finally the mass of proppants and clean liquid required for each stage can be obtained using the following equations.

$$V_{stage} = q_i (1 - \frac{c_{added}}{\rho_p}) \quad \text{……..……..……..……..... (1.41)}$$

$$M_{prop,stage} = c_{added} V_{stage} \quad \text{……...……..……..……..... (1.42)}$$

The procedures to determine treatment schedule to achieve the fracture dimensions providing the maximum productivity index can be summarized in flow chart as illustrated in **Fig. 1.11.**

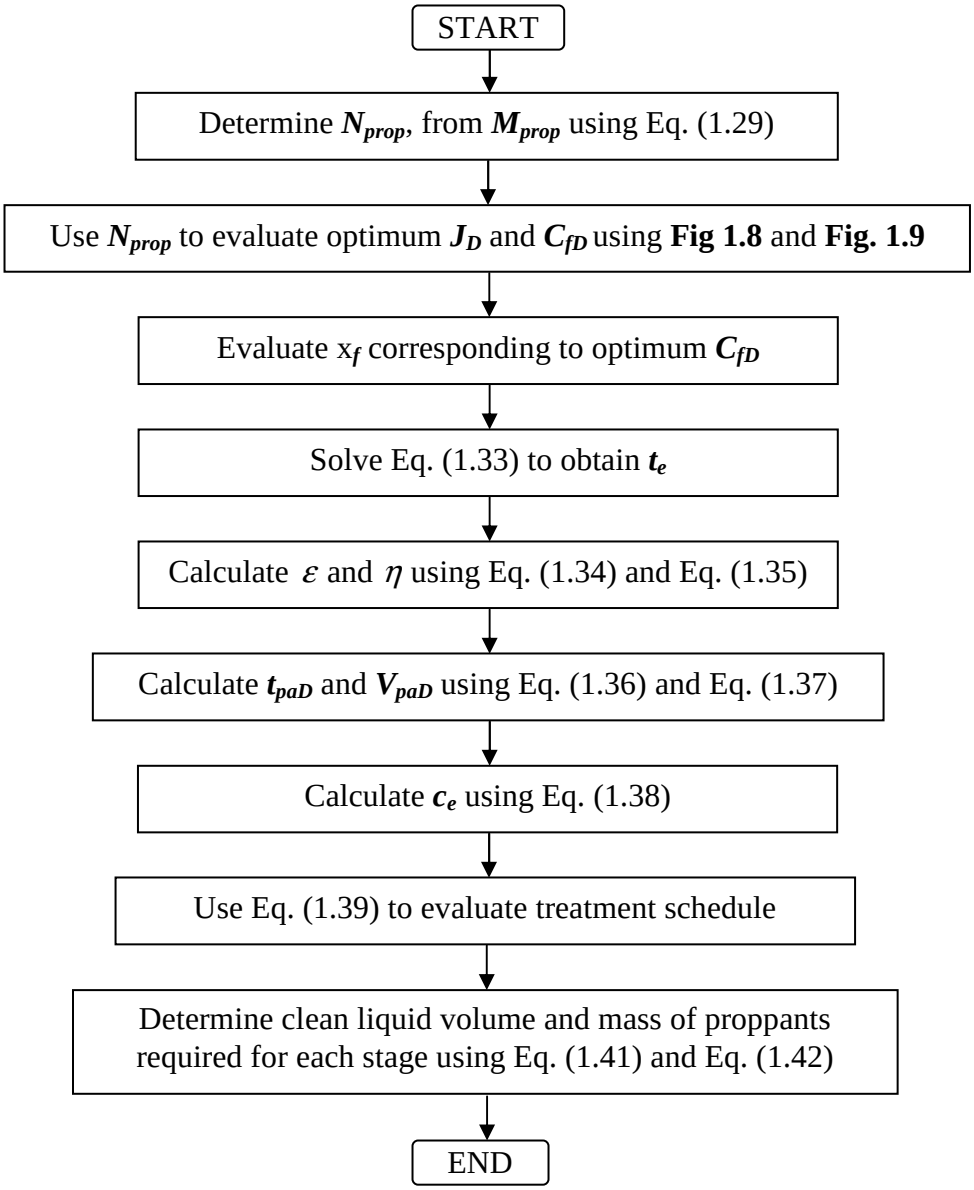

Fig. 1.11−Flow chart of treatment schedule determination based on fracture dimensions from UFD

1.1.5 Fracture Height Calculation

To determine a realistic fracture design, reasonable estimates of the fracture geometry must be obtained. Fracture half-length is determined based on the dimensionless fracture conductivity corresponding to the maximum productivity index. According the optimum fracture half-length, with the history of fracture fluid, the hydraulic fracture width can be calculated using 2D fracture propagation models, PKN and KGD models.

There is some evidence from production logs and other evaluation techniques suggesting that hydraulic fractures often terminate before propagating far into the bounding, impermeable layers. As a result, in order to help engineers determine the fracture design easier, the fracture height is assumed to be constant and equal to the gross pay height. However, this phenomenon happens only when the contrast of some properties of the reservoirs rock and bounding formation, such as minimum in-situ stress and Young's modulus, are very high or interface slippage occurs. Presence of interface slippage can result in immediate fracture growth termination.

Anderson (1981), and Teufel and Clark (1984) found that the interface containment is controlled by the frictional shear stress acting on the interface plane. When the frictional force is small, the tensional stress cannot be easily transmitted across the interface and slippage is likely to occur. It results in the fracture growth is terminated at the interface. On the other hand, when frictional force is large, the interface is transparent and stress is readily transmitted across it. The frictional shear stress, as described in Eq. (1.43), depends on the effective normal stress acting on interface. From

the equation, it can be said that shear slippage is likely to occur only where the frictional shear stress is small.

$$\tau = \mu_f \sigma_n \quad \text{……..…….……..…….....} \quad (1.43)$$

Because the interfaces are generally horizontal, the normal stress is usually equal to the overburden. Under normal situation, this is likely only at very shallow depth where the overburden stress is small. Most petroleum reservoirs, however, are at the great depth. It is hard for interface slippage occurring in petroleum fields.

As a result, it can be said that if the contrast of properties of the reservoirs rock and bounding formation are not very high or interface slippage does not occur, the fracture height assumed to be equal to gross pay is not accurate because the fracture tends to grow into upper and lower bounding formation. The following will describe some theories that have been applied for fracture height determination. In addition, some examples of calculation will be provided.

Equilibrium height concept

Normally, once fracture is created in the target layer which commonly has the smallest minimum principal stress (perforated interval), the fracture grow upward and downward through the adjacent layers which have larger minimum stress. There are many researches explained the crack behaviors.

Griffith (1921) is the first person who introduced the credible theory of crack behavior. He attempted to analyze the cracks behavior in class under tensile-loading conditions. He assumed that the microcracks were elliptical with a small minor axis and

used an energy ascribed to the newly released crack surface energy. For an elliptical crack in plane strain under a simple tensile-loading condition, the work to extend a crack of half-height, *a*, by an amount *da* is given by

$$dW = \frac{-\pi\sigma\left(1-\nu^2\right)}{E} a\,da \quad \text{..... (1.44)}$$

where dW is equated to the newly released surface energy (for two new faces):

$$dW = 2\gamma_W\, da \quad \text{..... (1.45)}$$

where γ_W is the surface energy. Now, a critical stress value for crack growth can be solved by

$$\sigma_c = \sqrt{\frac{2E\gamma_W}{\pi\left(1-\nu^2\right)a}} \quad \text{..... (1.46)}$$

Barenblatt (1962) had an opinion that Griffith's theory was inadequate because an overall elliptical fracture shape leads to unrealistic infinite stresses at the crack tip for uniformly loaded cracks in equilibrium. He proposed a model leading to the same crack-extension criterion while eliminating the singularity at the crack tip. He recognized that there would be very large, attractive molecular forces (cohesive forces) at the crack tip. These forces act in small area near the crack tip and would tend to pull the crack faces together. Considering the moment without external loading, the cohesive forces, compressive in nature, would result in stress singularity at the tip. Then, he introduced his theory that this compressive stress singularity is equal to the tensile stress singularity at the edge of the cohesion zone so that the effects cancel and no singularity occurs.

He introduced a new property of material called the modulus of cohesion, K'. He ascribed all the work of the cohesive modulus to surface energy as

$$K' = \sqrt{\frac{\pi E \gamma_W}{\left(1-\nu^2\right)}} \quad \text{.....} \quad (1.47)$$

Under simple loading conditions of uniform pressure in the crack,

$$\frac{K'}{\pi} = \sigma\sqrt{\frac{a}{2}} \quad \text{.....} \quad (1.48)$$

So, a critical stress value for crack growth can be solved by

$$\sigma_c = \frac{K'}{\pi}\sqrt{\frac{2}{a}} = \sqrt{\frac{2E\gamma_W}{\pi\left(1-\nu^2\right)a}} \quad \text{.....} \quad (1.49)$$

This is equivalent to the Griffith criteria.

Linear elastic fracture mechanics (LEFM) is related to Griffith's theory, but was modified by Orowan (1952) and restated by Irwin (1957) to include dissipative energy processes. LEFM states that a fracture will advance when its stress intensity reaches a critical value, K_{IC}, assuming that the crack tip is in a state of plane strain. K_{IC} is known as the plane-strain fracture toughness and has been shown to be measurable material property.

Irwin (1957) classified three different singular stress fields according to the displacement. Mode I is opening, Mode II is in-plane sliding (shearing), and Mode III is anti-plane sliding of crack (tearing). For hydraulic fracturing problem, only the opening mode is involved and stress intensity respecting to Mode I is denoted by K_I.

Rice (1968) derived an expression to calculate Mode I stress intensity factor for a crack extending from $-a$ to $+a$ on the y axis as shown in **Fig. 1.12**.

$$K_I = \frac{1}{\sqrt{\pi a}} \int_{-a}^{a} p(y_m) \sqrt{\frac{a + y_m}{a - y_m}} dy_m \quad \text{..... (1.50)}$$

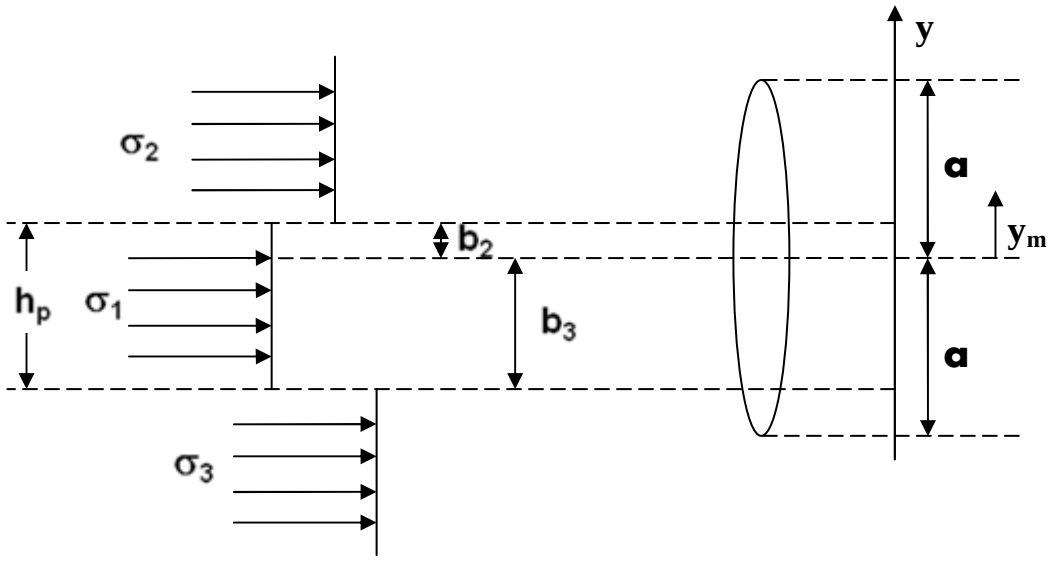

Fig. 1.12−Notation for fracture height calculation (non-dimensionless system)

The fracture height calculation procedure was proposed by Simonson et al. (1978) for a symmetric geometry, but is easily generalized to more complex situations. Basically, the method aims at the calculation of the equilibrium height of the hydraulic fracture for a give internal pressure in a layered-stress environment. The equilibrium height satisfies the condition that the computed stress intensity factors at the vertical tips (top and bottom) are equal to fracture toughness of the layer as illustrated in **Fig. 1.13**.

$$K_I = K_{IC} \quad \text{..... (1.51)}$$

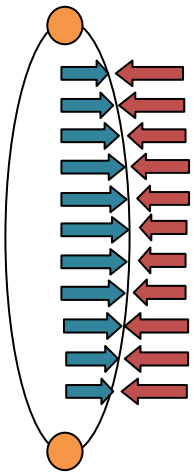

Fig. 1.13−Stress intensity at the tips are equal to fracture toughness of the layer

Fig. 1.14 illustrates how the fracture occurs after fracturing operation in three layers system. It looks similar to **Fig 1.12** but **Fig. 1.14** is used to analyze and help us describe the fracture in dimensionless system. As a result, Eq. (1.51) which expresses **Fig 1.12** can be rewritten in dimensionless system.

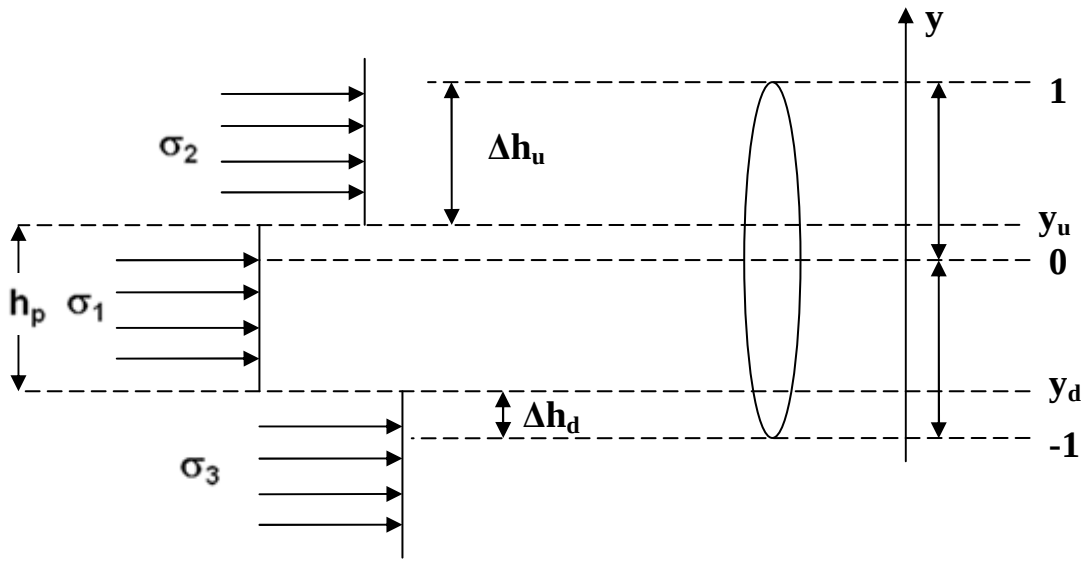

Fig. 1.14−Notation for fracture height calculation (dimensionless system)

Let *y* be the dimensionless vertical position:

$$y = \frac{y_m}{a} \quad \text{..... (1.52)}$$

$$dy_m = ady \quad \text{..... (1.53)}$$

Rewrite Eq. (1.51) in dimensionless system:

$$K_I = \sqrt{\frac{a}{\pi}} \times \int_{-1}^{1} p_n(y) \sqrt{\frac{1+y}{1-y}} dy \quad \text{..... (1.55)}$$

a is half-height in non-dimensionless system. It is equivalent to 1 in dimensionless system. Also, $y_u - y_d$ in dimensionless system is equivalent to h_p or height of perforation interval.

$$\frac{1}{a} = \frac{y_u - y_d}{h_p} \quad \text{..... (1.56)}$$

Substitute into Eq. (1.55):

$$K_{IC} = \sqrt{\frac{h_p}{\pi(y_u - y_d)}} \times \int_{-1}^{1} p_n(y) \sqrt{\frac{1+y}{1-y}} dy \quad \text{..... (1.57)}$$

According to **Fig. 1.14**, the middle layer commonly has the smallest minimum principle stress (σ_1). The two adjacent layers have larger minimum in-situ stress (σ_2, $\sigma_3 > \sigma_1$). As the pressure at the center of perforation increases, the equilibrium penetrations into the upper (Δh_u) and lower (Δh_d) layers increase. The requirement of equilibrium poses two constraints (stress intensity at both tips equal to fracture toughness), resulting in a system of two equations that can be solved simultaneously.

$$K_{IC2} = K_{I,Top} = \sqrt{\frac{h_p}{\pi(y_u - y_d)}} \times \int_{-1}^{1} p_n(y) \sqrt{\frac{1+y}{1-y}} dy \quad \text{..... (1.58)}$$

$$K_{IC3} = K_{I,Bottom} = \sqrt{\frac{h_p}{\pi(y_u - y_d)}} \times \int_{-1}^{1} p_n(y) \sqrt{\frac{1-y}{1+y}} dy \quad \text{..... (1.59)}$$

y_u, y_d are dimensionless vertical position of top and bottom perforation, respectively. (see **Fig. 1.14**)

$$y_u = \frac{\frac{h_p + \Delta h_u + \Delta h_d}{2} - \Delta h_u}{h_p + \Delta h_u + \Delta h_d} = 1 - \frac{2\Delta h_u}{h_p + \Delta h_u + \Delta h_d} \quad \text{..... (1.60)}$$

$$y_u = \frac{-\left(\frac{h_p + \Delta h_u + \Delta h_d}{2}\right) + \Delta h_d}{h_p + \Delta h_u + \Delta h_d} = -1 + \frac{2\Delta h_d}{h_p + \Delta h_u + \Delta h_d} \quad \text{..... (1.61)}$$

$p_n(y)$ in Eq. (1.43) and Eq. (1.44) represents the net pressure at any dimensionless vertical position, y. It can be described as the difference of treating pressure at that location and minimum in-situ stress of the layers. The treating pressure at any location is equated to the summation of pressure at the center of crack and hydrostatic pressure from the center of crack to that location. As a result, the net pressure distribution can be written as

$$p_n(y) = k_{00} + k_1 y - \sigma(y) \quad \text{..... (1.62)}$$

where k_{00} is pressure at the center of crack. Assuming the treating pressure at center of perforation, p_{cp}, is known, k_{00} can be calculated from the summation of p_{cp} and hydrostatic pressure from the center of perforation to the center of crack.

$$k_{00} = p_{cp} + \rho g \left(\frac{h_p}{y_u - y_d} \right) \left(\frac{y_u + y_d}{2} \right) \quad \text{.....} \quad (1.63)$$

where $\left(\frac{y_u + y_d}{2} \right)$ is the dimensionless position of center of perforation and

$\left(\frac{h_p}{y_u - y_d} \right)$ is a factor to convert dimensionless to non-dimensionless system.

k_1 in Eq. (1.62) represents the hydrostatic gradient.

$$k_1 = -\rho g \frac{h_p}{y_u - y_d} \quad \text{.....} \quad (1.64)$$

Solving two constraints, Eq. (1.58) and Eq. (1.59), dimensionless position of top and bottom of perforation, y_u, y_d, will be obtained. Consequently, the equilibrium penetrations into the upper (Δh_u) and lower (Δh_d) layers can be calculated. The fracture height can be computed using Eq. (1.65)

$$h_f = h_p + \Delta h_u + \Delta h_d \quad \text{.....} \quad (1.65)$$

The example of fracture height calculation is shown as the following. Fracture is created with 5 ppg of concentration of proppant, and 3250 psi of treating pressure at center of perforation. The gross pay height (perforated interval) is 180 ft. The minimum in-situ stress of target layer, top and bottom bounding formations are 3060, 3560, and

3560 psi, respectively. Fracture toughness of the top and bottom bounding layers are the same and equal to 1000 $psi/\sqrt{inch}$.

In order to solve the equilibrium height equation system, it requires iterative solution of two equations, Eq. (1.58) and Eq. (1.59). In this research, *Mathematica* was mainly used to solve the problem. For this problem, the solution is that the dimensionless position of top and bottom of perforation are 0.903 and -0.781, the equilibrium penetrations into the upper and lower layers are 10.4 and 23.4 ft., and total fracture height is 213.7 ft.

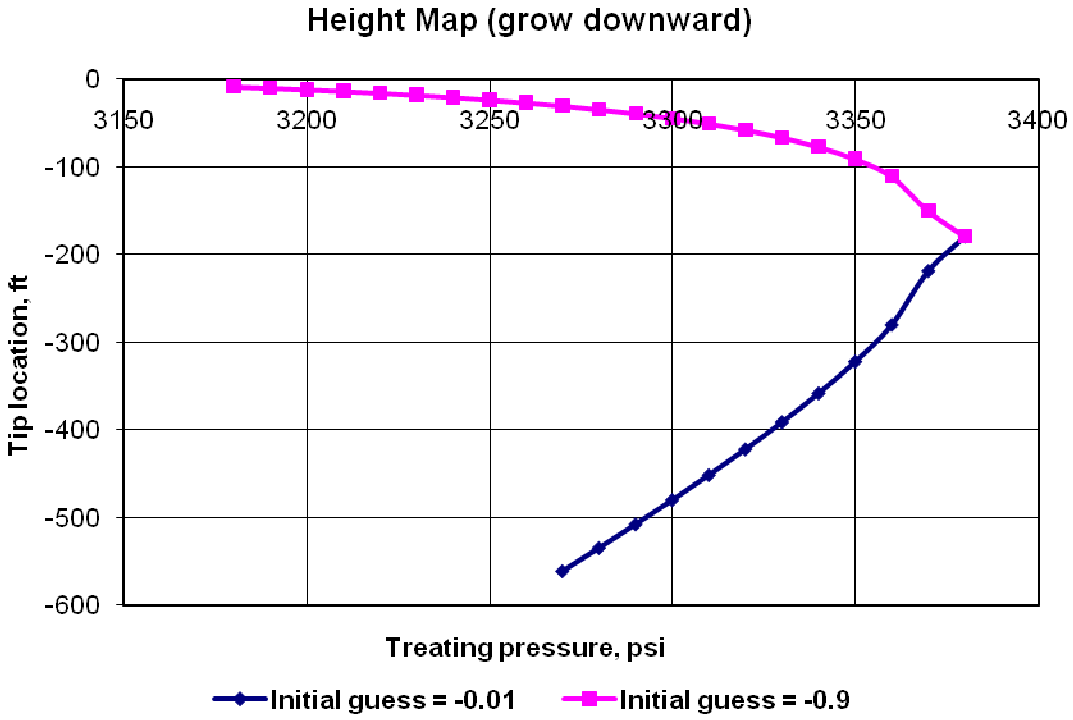

Fig. 1.15−Height map penetrating into lower layer

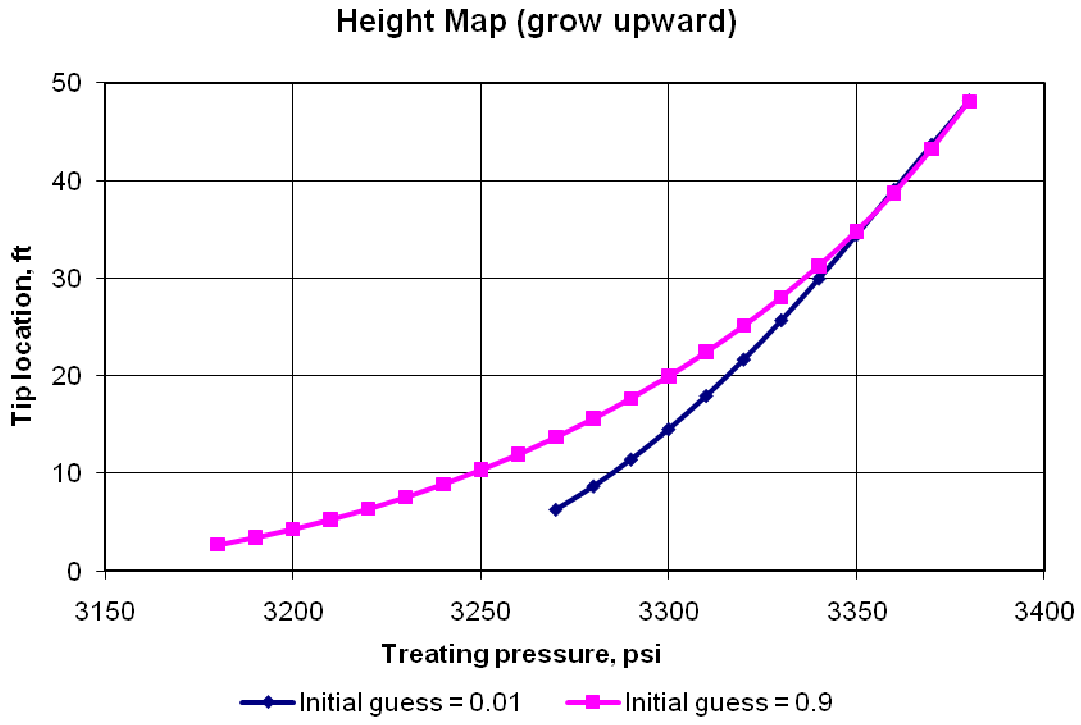

Fig. 1.16−Height map penetrating into upper layer

However, the equilibrium height can give rise to multiple solutions at some bottomhole pressure. Both figures are examples of height map obtained from the equilibrium height. **Fig. 1.15** and **Fig. 1.16** were generated by varying the treating pressure at center of perforation with the same reservoir, rock and fluid properties as shown in previous example.

Fig. 1.15 illustrates fracture growth downward and **Fig. 1.16** illustrates fracture growth upward. According to this example, if the pumping pressure is higher than 3270 psi, there will be occurring of multiple solutions. These multiple solutions are resulted from different initial guesses. The pink lines (top lines) in both figures are the results from initial guess value of y_u and y_d equal 0.01 and -0.01, respectively whereas the

blue lines (bottom lines) are the results from initial guess equal 0.9 and -0.9. As a result, some other methods are applied to determine the fracture height instead of equilibrium height concept when treating pressure at center of center of perforation is out of range of stability of solution. It will be explained in detail in the methodology part.

According to Eq. (1.47), Eq. (1.48), and Eq. (1.49), the net pressure distribution is a function of pressure at the center of crack, k_{00}. In reality, during the design process, pressure at the center of crack is unknown. However, it can be derived by the summation of the net pressure at the center of crack, p_{nw}, and minimum in-situ stress of the target layer, σ_h.

$$k_{00} = p_{nw} + \sigma_h \quad \text{……...……..……..……} \quad (1.66)$$

Net pressure is the product of fracture stiffness and the hydraulic fracture width. So the net pressure at the center of crack can be obtained from

$$p_{nw} = S_f w_{w,0} \quad \text{……...……...……..……..……} \quad (1.67)$$

1.2 Problem Description

The productivity index is a parameter to measure the reservoir performance. A good fracture design is resulting in the optimum productivity index after stimulation treatment. In general, the fracture designs must provide important information for the treatment, which are proppant concentration schedule, volume of clean liquid and amount of proppants required for each pumping stage. As a result, in order to determine

a realistic fracture design, reasonable estimates of fracture geometry; fracture half-length, width, and height, is essential.

The fracture half-length and the propped fracture width can be determined from the dimensionless fracture conductivity index corresponding to the maximum productivity index. PKN and KGD models are used to evaluate the hydraulic fracture width from calculated fracture half-length. Both of fracture half-length and fracture width determination require fracture height as an input.

LEFM is used to explain fracture growth in vertical direction. In this study, equilibrium height requiring that stress intensity at the vertical tips are equal to fracture toughness of the layers is applied for the fracture height calculation. However, the calculation requires the knowledge of net pressure distribution which is derived from treating pressure at the center of crack and it can be calculated from the hydraulic fracture width which is an output of the fracture design.

It can be concluded that the fracture height is required as an input of the fracture design; however, the fracture height itself is evaluated from the net pressure which is an output of the fracture design. As a result, it is necessary to apply numerical method to incorporate fracture height determination into unified fracture design.

1.3 Research Objective

This research improves the current unified fracture design. Equilibrium height will provide more reasonable estimation of fracture height which is required as an input

of the unified fracture design. Bisection method is applied to incorporate the rigorous height calculation using equilibrium height into the unified fracture design.

Although, equilibrium height is a reasonable concept to estimate fracture height. At specific stress contrast between target layer and bounding formations, this concept provides unique solutions only for a limited range of net pressures. This range is dependent on the stress contrast. This would cause a limitation of this approach. The problem is that when stress contrast is too high or too low, the convergence of the couple procedure deteriorates or does not happen at all. This research will provide other additional assumptions to make this approach applicable to any reservoir conditions.

CHAPTER II

METHODOLOGY

2.1 Incorporating Equilibrium Height into Unified Fracture Design

From the literature review part, it is known that in order to solve the equilibrium height equation system, it would require iterative solution of two equations, Eq. (1.58) and Eq. (1.59) which are the function of net pressure distribution. *Mathematica* is employed to obtain the final solution or fracture height. The net pressure can be obtained from the fracture design where the fracture design requires fracture height as an input parameter. As a result, in this research, bisection method is applied to incorporate the rigorous height calculation using equilibrium height into the unified fracture design.

In this section, an example is given to illustrate an idea how bisection method help us solve the problem. The example shows the determination of fracture height after fracturing in tight reservoir (0.35 md). Reservoir drainage area, net pay and gross pay thickness are 40 acre, 70 ft and 180 ft, respectively. The target layer has 3060 psi of closure stress and 2×10^6 psi of plane strain modulus. Both of upper and lower bounding layers have 3660 psi of closure stress and 1000 psi-in$^{0.5}$ of fracture toughness. The fracture will be created by 300000 lbm of proppants with 3.1 of proppant specific gravity. Proppant packed porosity with and without stress are 0.25 and 0.38, respectively. Fracture permeability is 30000 md. Injection rate of slurry is 30 bpm (two wings). The rheology properties of frac fluid are 0.45 of flow behavior index and 0.60 of consistency index. It is assumed that leak-off coefficient of net pay is 0.003 ft/min$^{0.5}$,

spurt loss is negligible and fluid loss in impermeable layers is half of that in pay zone. The input parameters of this example can be summarized as shown in **Table 2.1**.

TABLE 2.1−SUMMARY OF INPUT PARAMETERS FOR DEMONSTRATION OF USING BISECTION METHOD TO DETERMINE FRACTURE HEIGHT

Reservoir info.	
Permeability	0.35 md
Drainage area	40 acre
Net pay thickness	70 ft
Gross pay thickness (perforated interval)	180 ft
Rock properties	
Plane strain modulus	2×10^6 psi
$\Delta\sigma$	600 psi
K_{IC}	1000 psi-in$^{0.5}$
Closure stress	3060 psi
Proppant properties	
Total proppant mass	300,000 lbm
Proppant retained permeability	30,000 md
Specific gravity	3.1
Proppant packed porosity	0.38
Proppant packed porosity under closure stress	0.25
Fluid properties	
Rheology flow behavior index, n	0.45
Rheology consistency index, K	0.6 lbf $\times s^n$ / ft^2
Slurry rate	30 bpm
Leak-off coefficient in net pay	0.003 ft/min$^{0.5}$
Spurt loss	neglect
Fluid loss multiplier out of net pay	0.5

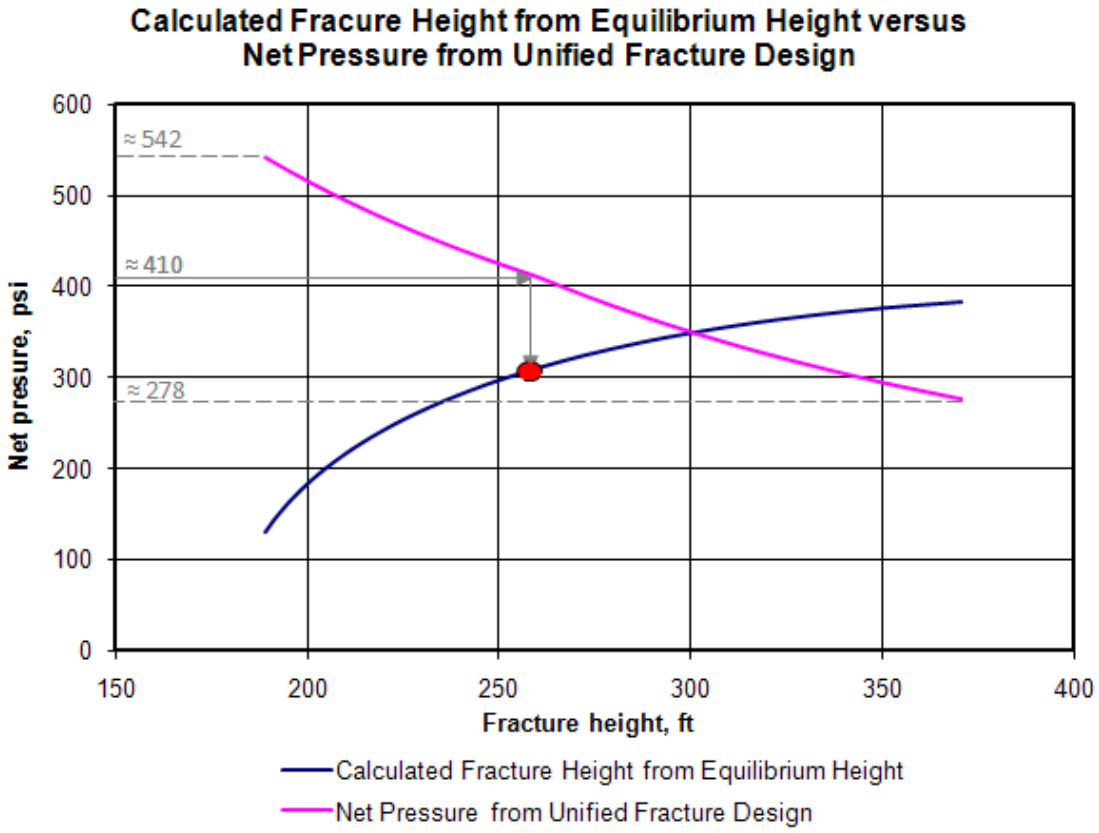

Fig. 2.1−The plot of calculated fracture height using equilibrium height (blue line) versus net pressure from fracture design (pink line). Both lines are generated respected to input parameters in Table 2.1

Using equilibrium height, the range of fracture height of this example which is corresponding to given net pressure (height map) can be created as shown as the blue line in **Fig. 2.1**. As mentioned, this concept is valid for only limited range of net pressure. In this case, the valid range of net pressure is approximately from 130 to 385 psi. With those calculated fracture heights, net pressure at the end of the job can be determined from the fracture design (pink line). The intersection of two lines represents the final solution or the fracture height.

In this research, bisection method is used to determine the solution and use it to evaluate the treatment schedule based on the fracture dimension obtained from unified fracture design. The step by step procedures to incorporate equilibrium height into unified fracture design are shown as the following:

i. Set the minimum and maximum of a range of net pressure in which the correct answer is supposed to be. For this example, according to the equilibrium height validation, the minimum and maximum net pressure determined by unified fracture design (pink line) are approximately 277 and 542 psi, respectively (see **Fig. 2.1**). However, in term of programming, it is not necessary to determine the valid range of net pressure to equilibrium height concept. In the program, the minimum net pressure is set to be equal to net pressure respected to upper limit of fracture height where fracture aspect ratio is equal to 1 (PKN model assumption) and the maximum net pressure is calculated from the lower limit of fracture height which is equal to thickness of perforation interval.

pn_{min} = *net pressure respected to the maximum fracture height* ..... (2.1)

pn_{max} = *net pressure respected to the minimum fracture height* ..... (2.3)

ii. Determine the average net pressure from the previous step. For this example, it is approximately 410 psi.

$$pn = \frac{pn_{\min} + pn_{\max}}{2} \quad \text{……..……..……..……..…..……} \quad (2.3)$$

iii. Evaluate fracture height from average net pressure using equilibrium height.

iv. Use the calculated fracture height to determine the net pressure from the fracture design (see red dot in **Fig. 2.1**).

v. Observe the calculated net pressure. If it is higher than the average net pressure from the second step, the average net pressure must set to be new minimum value whereas the maximum remains the same. On the other hand, if it is lower than the average net pressure, the average net pressure must set to be new maximum value.

vi. Repeat step (ii) to (v) for 16 times. (If the solution converges, the error will be less than 10^{-6}).

vii. Use the final solution (fracture height) to determine fracture dimensions using UFD and evaluate the treatment schedule.

The suggested procedures of incorporating equilibrium height into unified fracture design can be summarized in a flow chart as illustrated in **Fig. 2.2.**

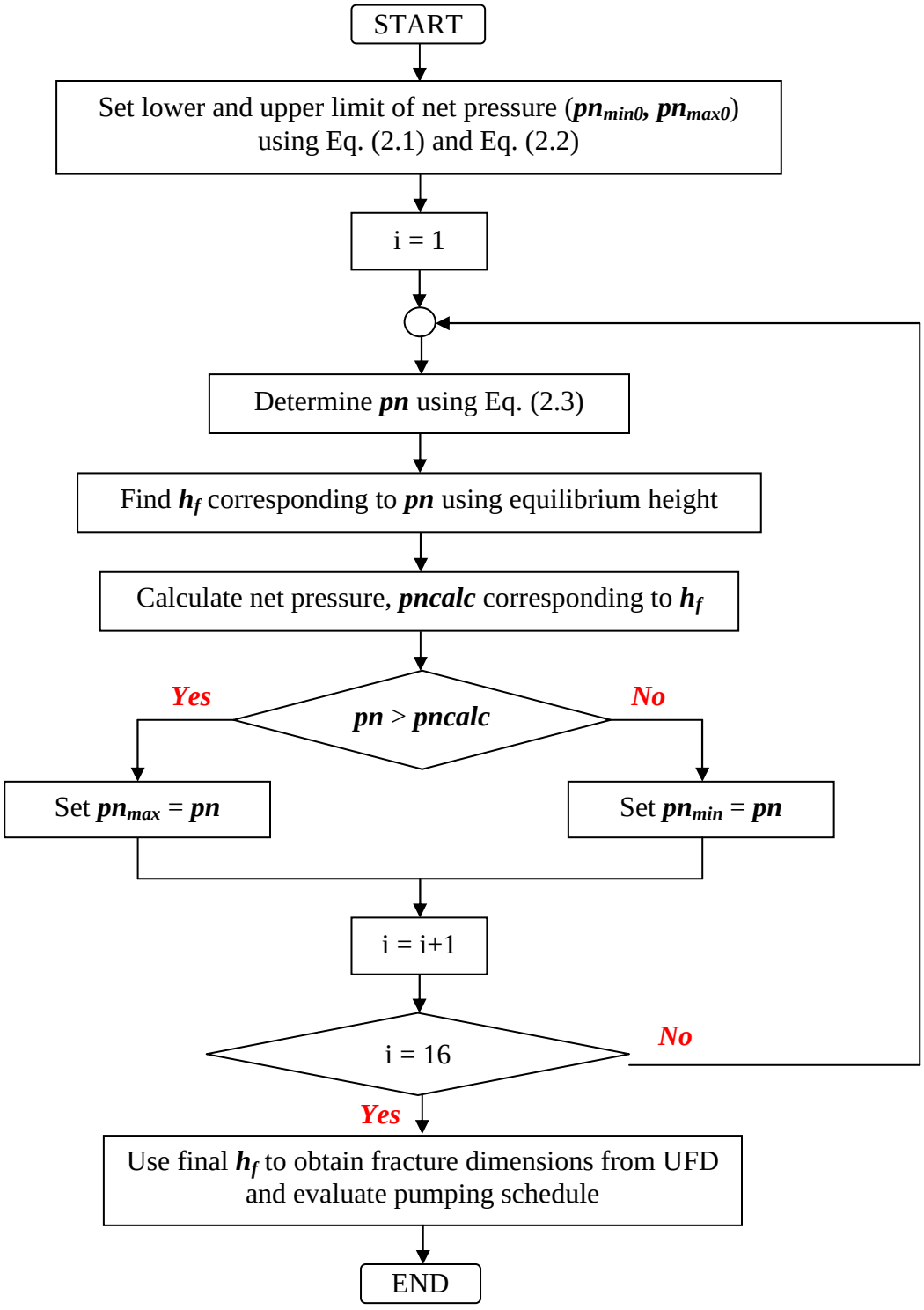

Fig. 2.2−Incorporating equilibrium height into unified fracture design

However, as mentioned, equilibrium height is valid for only limited range of net pressure (derived from the stress contrast between target layer and bounding formations). As a result, only this concept is not enough to make this approach applicable in a wide range of input data. It is necessary to make additional assumptions to safeguard the calculation in order to compensate for the fact that "equilibrium height" is unrealistic or may not exist at all. In the next section, those assumptions will be discussed.

2.2 Assumptions to Eliminate Height Calculation Constraint

In this section, some assumptions are made to determine fracture height in case that the equilibrium height is not applicable.

2.2.1 Simplify Equilibrium Height Equation System

The first assumption is that fracture growths upward and downward are equal. This can help us simplify the equilibrium height equation system from 2 equations 2 unknowns (y_d and y_u) to 1 equation 1 unknown (y_e) where

$$y_d = -y_e \quad \text{(2.4)}$$

$$y_u = y_e \quad \text{(2.5)}$$

Recall the equilibrium height equations:

$$K_{IC2} = K_{I,Top} = \sqrt{\frac{h_p}{\pi(y_u - y_d)}} \times \int_{-1}^{1} p_n(y) \sqrt{\frac{1+y}{1-y}} dy \quad \text{(2.6)}$$

$$K_{IC3} = K_{I,Bottom} = \sqrt{\frac{h_p}{\pi(y_u - y_d)}} \times \int_{-1}^{1} p_n(y) \sqrt{\frac{1-y}{1+y}} dy \quad \text{……...…} \quad (2.7)$$

Substitute y_d and y_u by Eq. (2.4) and Eq. (2.5) into the equilibrium height equations and add both of them together:

$$K_{I,Bottom} + K_{I,Top} = 2 \times \left(\sqrt{\frac{h_p}{2\pi y_e}} \times \int_{-1}^{1} p_n(y) \sqrt{\frac{1-y}{1+y}} dy \right) \quad \text{……...…} \quad (2.8)$$

Fracture height can be approximated from Eq. (2.8). *Mathematica* is used to obtain the iterative solution. This equation system is less complicated than the original one. As a result, the extension of the range of valid net pressure for calculation is possible. In other words, in case that the equilibrium height cannot determine the solution because it is out of the valid range of net pressure, the simplified equation will be used to approximate the solution. Nevertheless, this equation is derived from the equilibrium height. Thus, it has the same constraint as the original does.

2.2.2 Other Assumptions

As mentioned, both of the equilibrium height and its simplified version are valid for only limited range of net pressure. It can be implied that these are also limited for limited range of stress contrast (input data). As a result, the stress differences of target layers and bounding formations are considered as proper parameters for solving the problem. Thus, in case that both of the original and simplified equilibrium height are not applicable, fracture height will be determined based on the assumption that the net

pressure at the end of the job is equal to the average stress difference of the reservoir and adjacent layers. The average stress difference is:

$$\Delta\sigma_{avg} = \frac{\sigma_{Top} + \sigma_{Bottom} - 2\sigma_{mid}}{2} \quad \text{.....} \quad (2.9)$$

According to the literature review section, the fracture design can evaluate net pressure by given fracture height. In order to satisfy the above assumption, iterative calculation is necessary. *Mathematica* is used to perform the calculation until the net pressure at the end of the job is equal to the average stress difference using add-in fracture design.

Regarding PKN model derivation, it satisfies the vertical plane strain condition where fracture length is approximately greater than fracture height. Thus, the fracture aspect ratio; the ratio of fracture length to fracture height, must be greater than 1.

$$asp = \frac{2x_f}{h_f} > 1 \quad \text{.....} \quad (2.10)$$

Therefore, if the solution obtained from the calculation has the fracture aspect ratio greater than 1. It is necessary to recalculate the fracture height based on the assumption that the fracture aspect ratio equal to 1.

2.3 Summary of Procedures

The procedures of incorporating rigorous height determination into unified fracture design can be concluded as the following:

i. Start with computing of upper limit of net pressure, $\boldsymbol{pn_{max0}}$, from minimum fracture height or gross pay thickness and lower limit of net pressure, $\boldsymbol{pn_{min0}}$, from maximum fracture height where fracture aspect ratio is equal to 1 using unified fracture design. Then, determine fracture height, $\boldsymbol{h_f}$, respected to $\boldsymbol{pn_{max0}}$ and $\boldsymbol{pn_{min0}}$ using equilibrium height.

ii. Use $\boldsymbol{h_f}$ from previous step to determine new net pressure and check that if the value is greater than $\boldsymbol{pn_{max0}}$ or less than $\boldsymbol{pn_{min0}}$ or not. If yes, it implied that the final solution cannot be obtained from the original equilibrium height and go to step (iv). If not, go to next step.

iii. Determine the iterative solution using bisection method as explained in **Sect. 2.1 (Fig. 2.2)**. In this research, function called *FindMinimum* in *Mathematica* is used to evaluate whether if the solution obtained by iterative calculation is converged or not by returning one of the output which is assigned to be called ***Objfun***. This parameter identifies an error of the calculation. For this program, the acceptable error of calculation must be less than 10^{-3}. In other words, if the value of ***Objfun*** is less than 10^{-3}, it represents that the convergence of the solution exists. If the solution can be obtained by the original equilibrium height, go to step (vi). If not, go to next step.

iv. Determine the solution by simplified equation of equilibrium height with the same procedure as the original one's and observe convergence of the solution. If the solution converges, go to step (vi). If not, go to next step.

v. Determine the solution based on assumption that the net pressure at the end of the job is equal to the average stress contrast between the target layers and bounding formations.

vi. Check the fracture aspect ratio of the solution from step (iii), (iv) or (v). If the aspect ratio is less than 1, re-calculate fracture height where the aspect ratio is equal to 1.

vii. Apply the final solution to the unified fracture design program to obtain the fracture dimensions. Then, determine the pumping schedule.

Flow chart of the summary of the procedures can be illustrated as shown in **Fig. 2.3**.

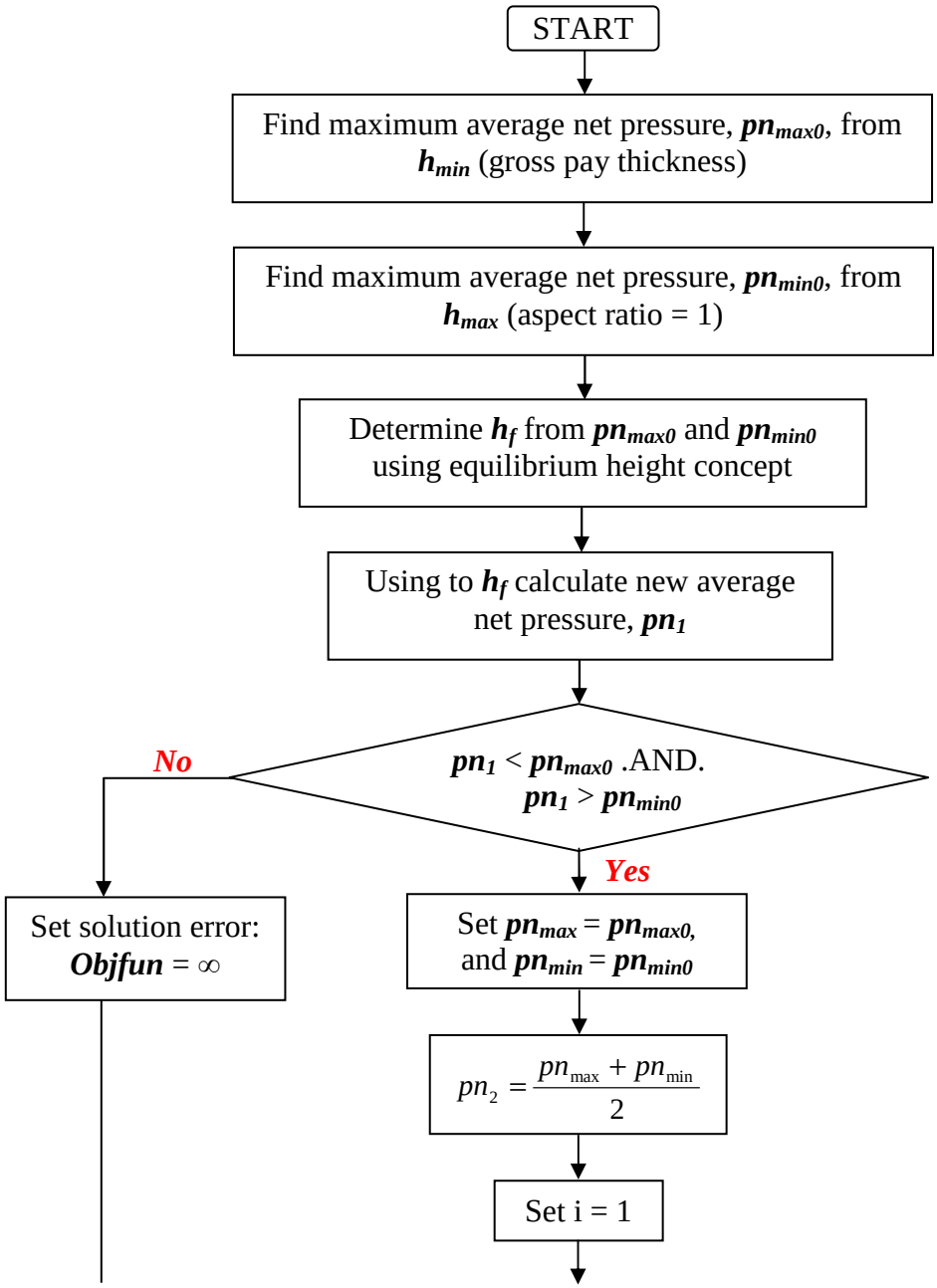

Fig. 2.3−Summary of procedures of incorporating rigorous height determination into unified fracture design

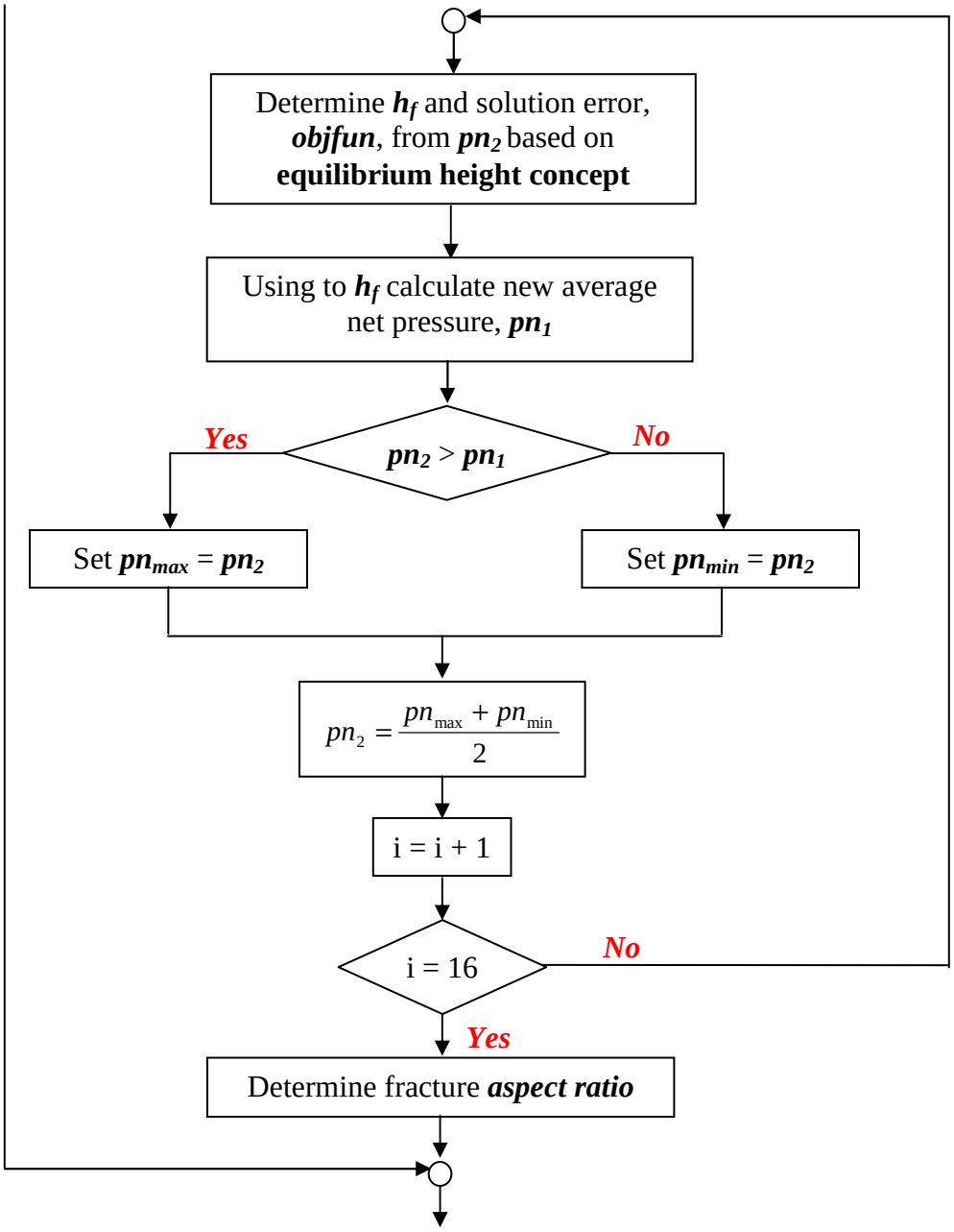

Fig. 2.3−Continued

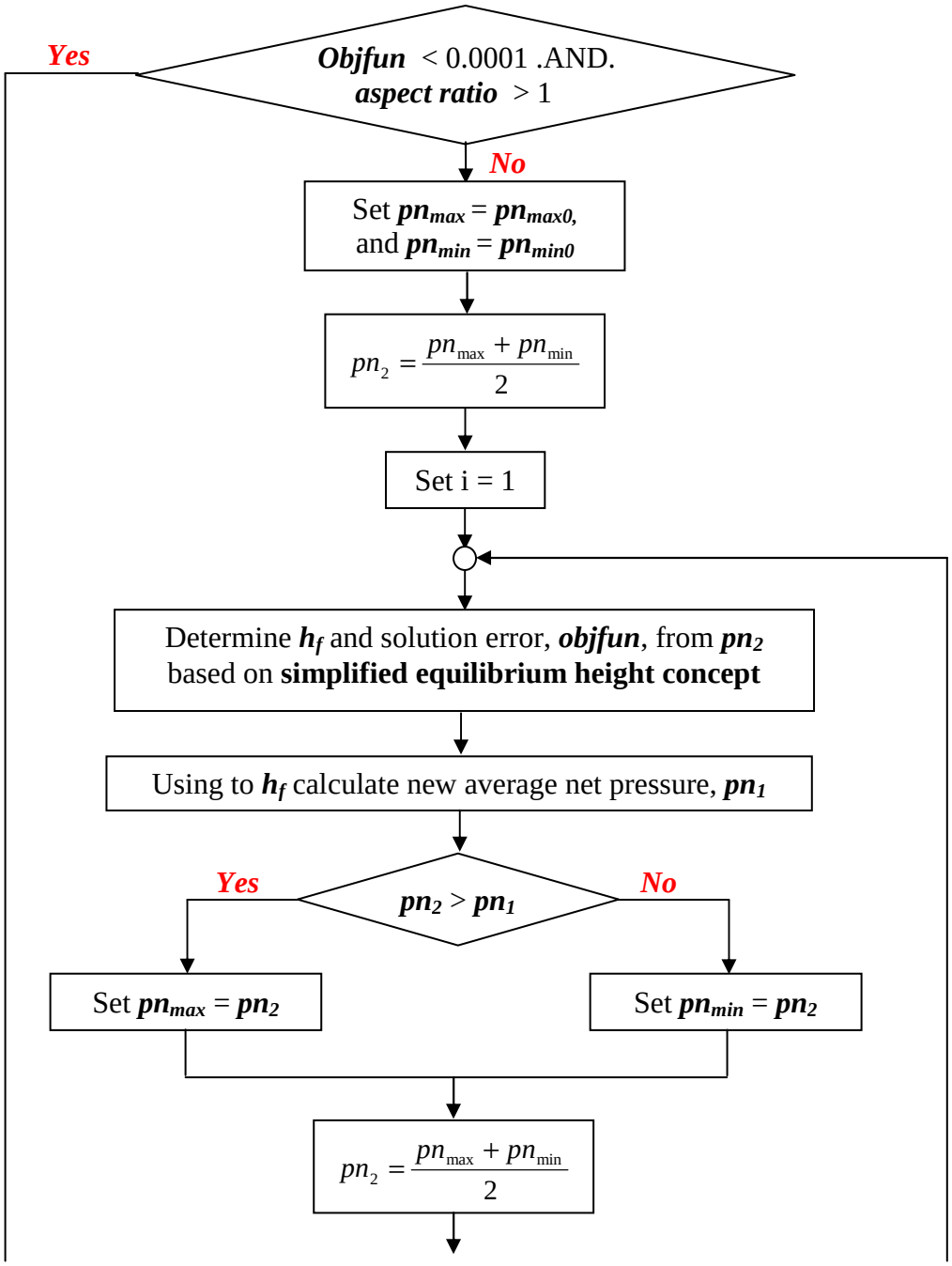

Fig. 2.3−Continued

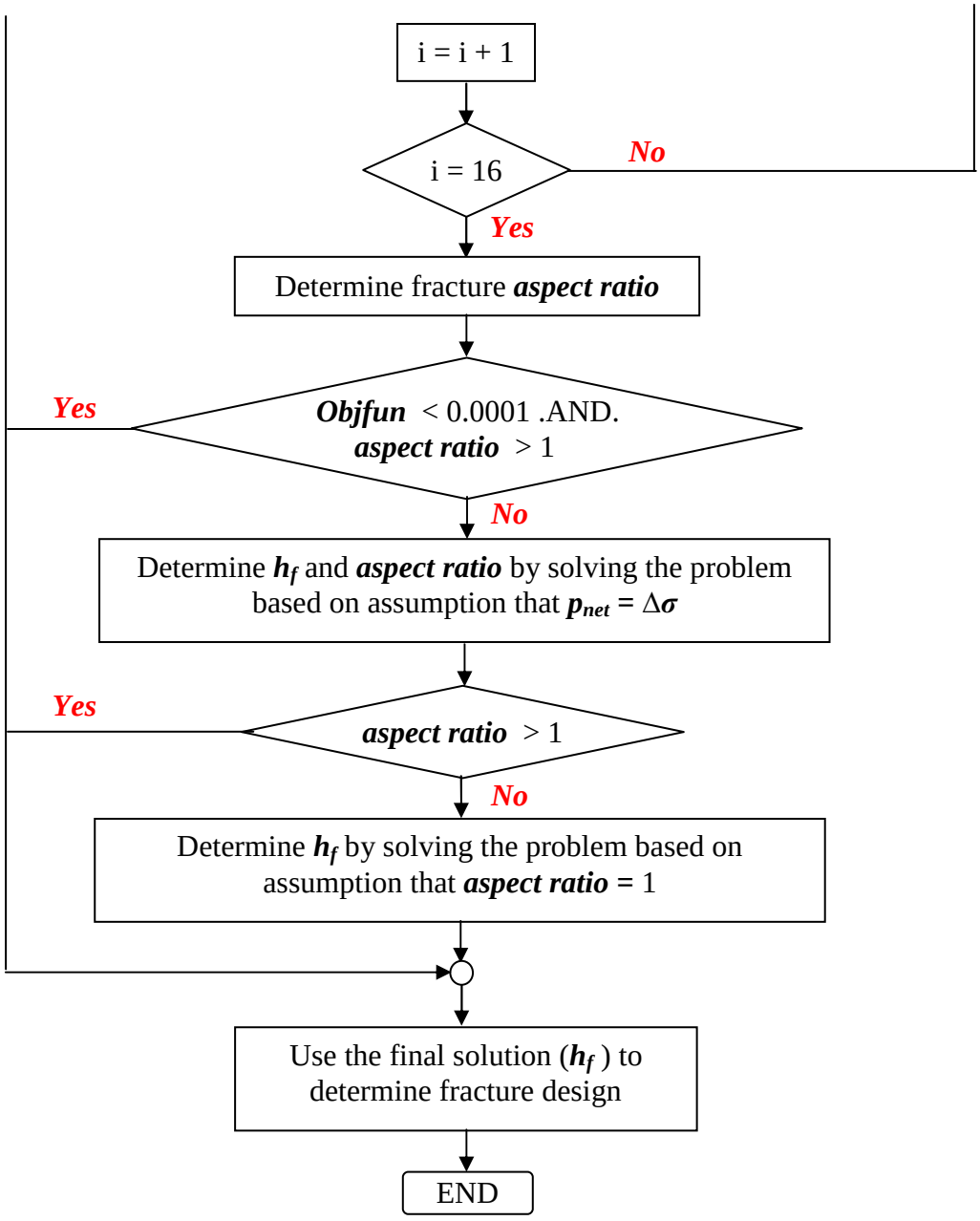

Fig. 2.3−Continued

CHAPTER III

APPLICATIONS AND DISCUSSIONS

3.1 Applications and Results from Add-in Fracture Design Program

In the first part of this section, five different sets of input parameters were used to demonstrate results from incorporating rigorous height calculation into the unified fracture design and determine treatment schedule based on the results. Each example (output) was evaluated based on different methods to determine fracture height:

i. Original equilibrium height (solving for fracture growths upward (y_u) and downward (y_d))

ii. Simplified equilibrium height (assuming that fracture growths upward and downward are equal ($y_u = y_d$))

iii. Assumption that the net pressure at the end of the job equals to the average stress difference of the reservoir and adjacent layers ($p_{net} = \Delta\sigma$)

iv. Assumption that the fracture aspect ratio is equal to 1 (in case that the final solution from above methods giving the aspect ratio less than one)

All of four cases have the same reservoir, proppant and fracture fluid properties. The designs were determined for hydraulic fracturing in tight reservoir (1.0 md). Reservoir drainage area is 40 acres. Net and gross pay thickness are the same which is equal to 250 ft. The fracture will be created by 500000 lbm of proppants with 3.3 of proppant specific gravity. Proppant packed porosity with and without stress are 0.25 and 0.38, respectively. Fracture permeability is 25000 md. Injection rate of slurry is 30 bpm

(two wings). The rheology properties of frac fluid are 0.45 of flow behavior index and 0.60 of consistency index. It is assumed that leak-off coefficient of net pay is 0.003 ft/min$^{0.5}$, spurt loss is negligible and fluid loss of bounding layers is half of that of pay zone. The input parameters of this example can be summarized as shown in **Table3.1**.

TABLE 3.1−SUMMARY OF RESERVOIR, PROPPANT AND FRAC FLUID PROPERTIES USED TO EVALUATE PUMPING SCHEDULES USING THE MODIFIED UNIFIED FRACTURE DESIGN PROGRAM FOR ALL CASES

Reservoir info.	
Permeability	1.0 md
Drainage area	40 acre
Net pay thickness	250 ft
Gross pay thickness (perforated interval)	250 ft
Proppant properties	
Total proppant mass	500,000 lbm
Proppant retained permeability	20,000 md
Specific gravity	3.3
Proppant packed porosity	0.38
Proppant packed porosity under closure stress	0.25
Fluid properties	
Rheology flow behavior index, n	0.45
Rheology consistency index, K	0.6 lbf ×s^n / ft^2
Slurry rate	30 bpm
Leakoff coefficient in net pay	0.003 ft/min$^{0.5}$
Spurt loss	neglect
Fluid loss multiplier out of net pay	0.5

As mentioned, the valid range of net pressure to determine fracture height using equilibrium height is limited. This range can be derived from the stress differences of target layer and adjacent formations. All the rock properties, apart from the stress

differences, of the target layer and the upper and lower bounding formations used for the first four examples are the same as shown in **Table 3.2**. . The target layer has 3000 psi of closure stress and 1.5×10^6 psi of plane strain modulus. Both of upper and lower bounding layers have 1000 psi-in$^{0.5}$ of fracture toughness.

TABLE 3.2−SUMMARY OF ROCK PROPERTIES USED TO EVALUATE PUMPING SCHEDULES USING THE MODIFIED UNIFIED FRACTURE DESIGN PROGRAM FOR ALL CASES

Rock properties	
Plane strain modulus	1.5×10^6 psi
K_{IC}	1000 psi-in$^{0.5}$
Closure stress	3000 psi

The stress differences ($\Delta\boldsymbol{\sigma_u}$ and $\Delta\boldsymbol{\sigma_d}$) were varied for each case to study the effect of those on the design obtain from the program. The stress differences used for each case are:

i. $\Delta\boldsymbol{\sigma_u}$ = 500 psi and $\Delta\boldsymbol{\sigma_d}$ = 500 psi,

ii. $\Delta\boldsymbol{\sigma_u}$ = 400 psi and $\Delta\boldsymbol{\sigma_d}$ = 150 psi,

iii. $\Delta\boldsymbol{\sigma_u}$ = 300 psi and $\Delta\boldsymbol{\sigma_d}$ = 150 psi and

iv. $\Delta\boldsymbol{\sigma_u}$ = 150 psi and $\Delta\boldsymbol{\sigma_d}$ = 150 psi

Case 1: $\Delta\sigma_u$ = 500 psi and $\Delta\sigma_d$ = 500 psi

In this example, the stress differences of the target layer and upper ($\Delta\boldsymbol{\sigma_u}$) and lower ($\Delta\boldsymbol{\sigma_d}$) bounding formations are the same and equal to 500 psi. The final solution of the fracture height is in the valid range of the original equilibrium height concept as shown in **Fig. 3.1**.

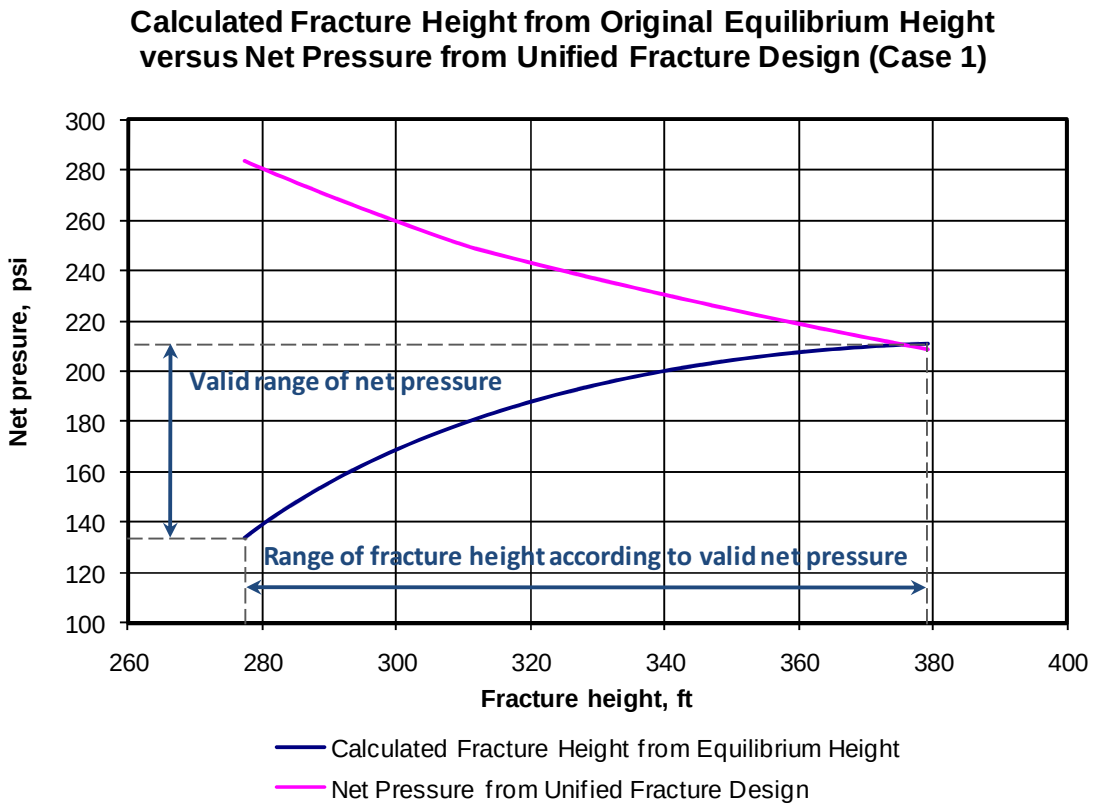

Fig. 3.1−The plot of calculated fracture height using original equilibrium height concept (blue line) versus net pressure from fracture design (pink line) for case 1. The final solution (the intersection) is in the valid range of calculation

The final solution (fracture height) obtained from the program is approximately 377.8 ft. The fracture dimensions obtained from the unified fracture design and the

treatment design including other important parameters for hydraulic fracturing operation based on calculated fracture dimensions was evaluated and shown in **Table 3.3**. The proppant concentration schedule, required proppant and clean liquid for each stage of pumping are shown in **Table 3.4** and **Fig. 3.2**. Fracture geometry at the end of the job is illustrated as **Fig. 3.3**.

TABLE 3.3−SUMMARY OF CALCULATED FRACTURE DIMENSIONS AND PARAMETERS FOR FRACTURE OPERATION FOR CASE 1

Fracture Dimensions	
Frac height, h_f (ft)	377.8
Frac half-length, x_f (ft)	262.0
Frac ave width, w_{ave} (in)	0.27
Hydraulic Fracturing Parameters	
Number of proppant, N_{prop}	0.27055
Dimensionless productivity index, J_D	0.604
Dimensionless fracture conductivity, FcD	1.717
Penetration ratio, I_x	0.3970
Slurry efficiency, η (%)	37.47
Prop. mass, M_{prop} (lbm)	500000
Clean fluid vol. (gal)	143807
Pumping time, t_e (min)	128.4
Net pressure (end time), p_{net} (psi)	209.7
Proppant conc. (end time), c_{add} (ppga)	11

TABLE 3.4−PUMPING SCHEDULE FOR CASE 1

	Start time (min)	End time (min)	c_{add} (ppga)	Proppant used (lbm)	Liquid used (gal)
Pad	0	58	0	0	73620
1	58	60	1	1740	1740
2	60	62	2	6090	3040
3	62	67	3	14240	4750
4	67	72	4	21570	5390
5	72	78	5	33220	6640
6	78	84	6	40820	6800
7	84	92	7	53980	7710
8	92	100	8	60350	7540
9	100	108	9	73940	8220
10	108	117	10	78370	7840
11	117	129	11	115690	10520

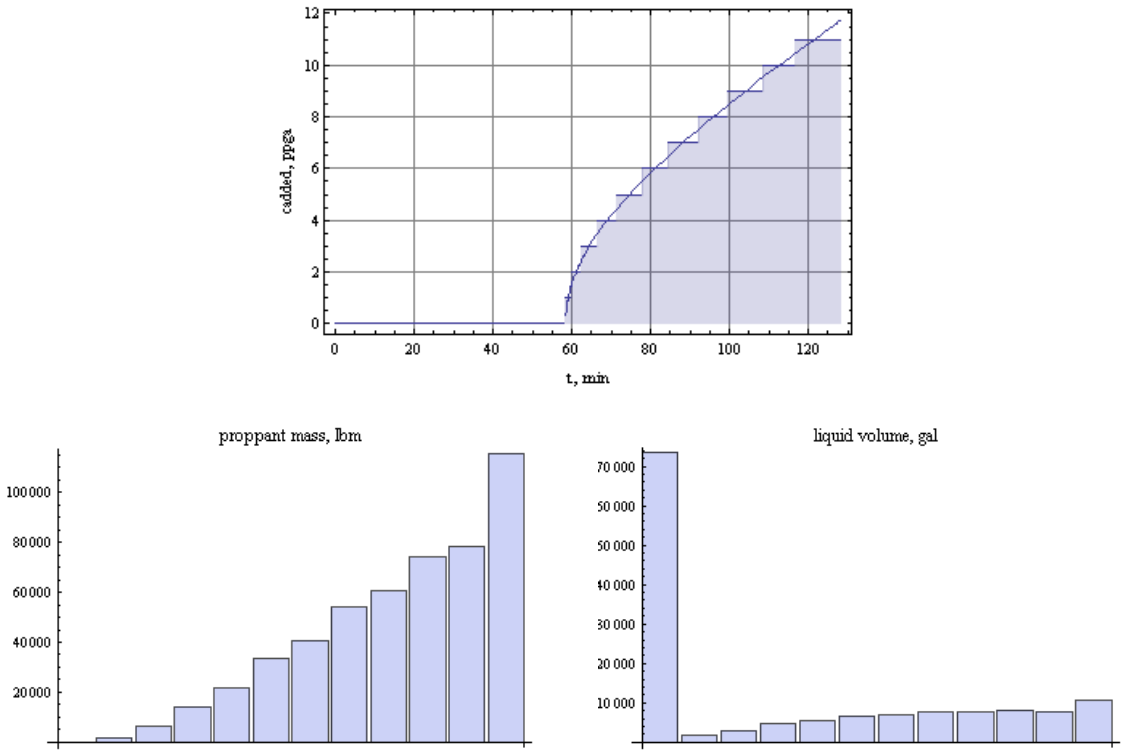

Fig. 3.2−(top) Proppant concentration schedule, (bottom left) amounts of proppants required for each stage, (bottom right) liquid volume used for each stage for case 1

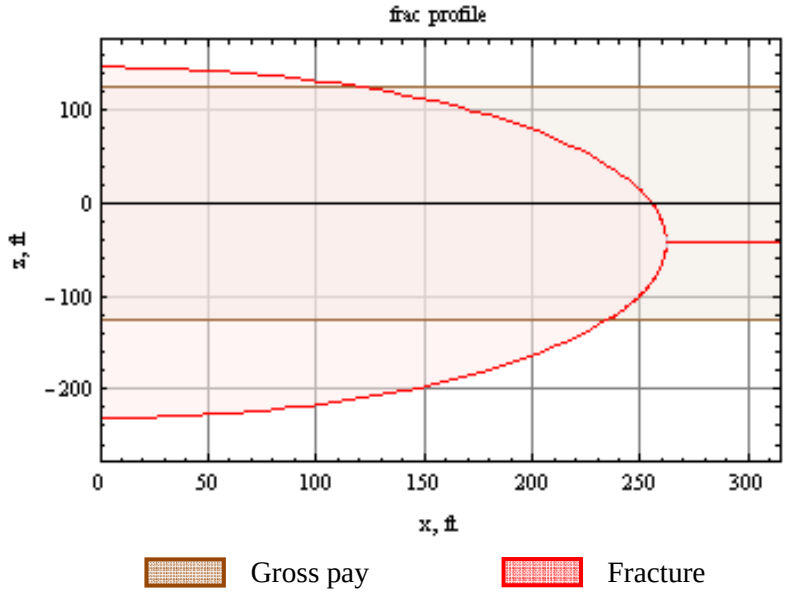

Fig. 3.3−Fracture geometry at the end of the job for case 1

Case 2: $\Delta\sigma_u$ = 400 psi and $\Delta\sigma_d$ = 150 psi

In this example, the stress differences of the target layer and upper and lower bounding formation ($\Delta\boldsymbol{\sigma_u}$, $\Delta\boldsymbol{\sigma_d}$) are 400 and 150 psi, respectively. The final solution of fracture height for this case is out of the valid range of original equilibrium height concept as shown in **Fig. 3.4**.

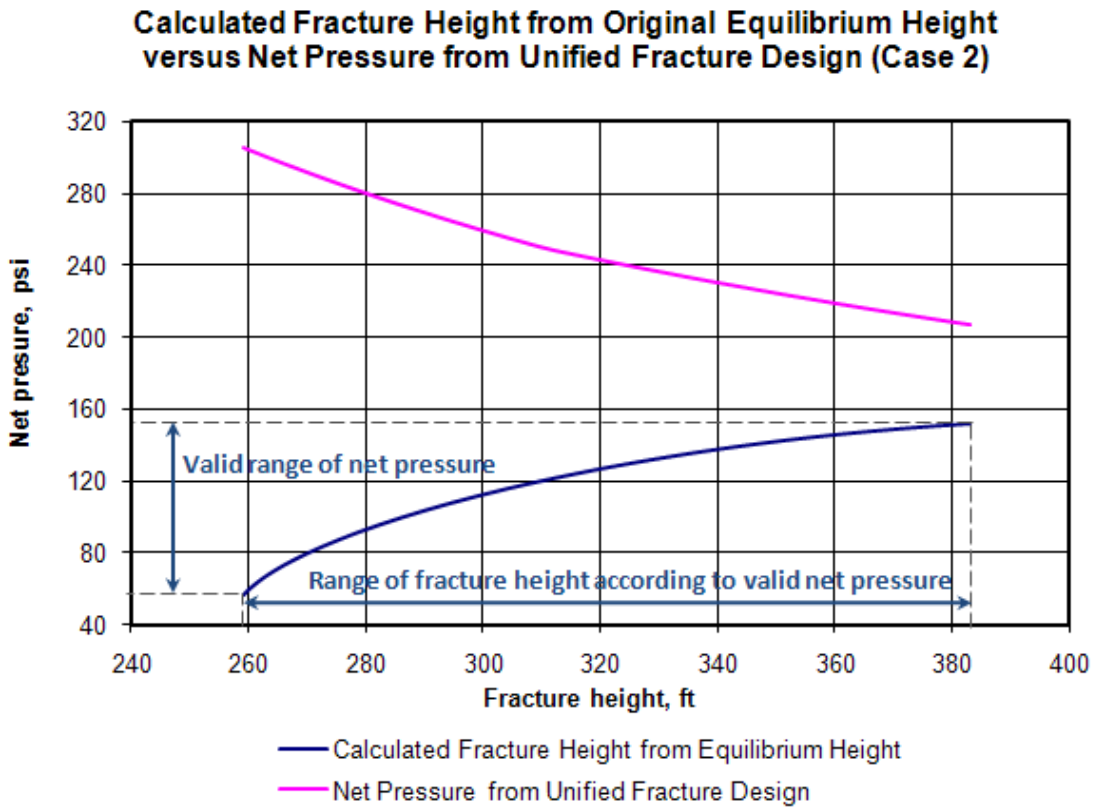

Fig. 3.4−The plot of calculated fracture height using original equilibrium height concept (blue line) versus net pressure from fracture design (pink line) for case 2. The final solution (the intersection) is out of the valid range of calculation

From figure above, in this case, the final solution (the intersection) is out of the valid range of original equilibrium height. As a result, the simplified equation is applied to determine the fracture height. It is approximately 476.6 ft.

The fracture dimensions and important parameters for hydraulic fracturing operation are shown in **Table 3.5**. The proppant concentration schedule, required proppant and clean liquid for each step of pumping are shown in **Table 3.6** and **Fig. 3.5**. Fracture geometry at the end of the job is illustrated as **Fig. 3.6**.

TABLE 3.5− SUMMARY OF CALCULATED FRACTURE DIMENSIONS AND PARAMETERS FOR FRACTURE OPERATION FOR CASE 2

Fracture Dimensions	
Frac height, h_f (ft)	476.6
Frac half-length, x_f (ft)	243.3
Frac ave width, w_{ave} (in)	0.25
Hydraulic Fracturing Parameters	
Number of proppant, N_{prop}	0.22901
Dimensionless productivity index, J_D	0.577
Dimensionless fracture conductivity, FcD	1.685
Penetration ratio, I_x	0.3686
Slurry efficiency, η (%)	37.89
Prop. mass, M_{prop} (lbm)	500000
Clean fluid vol. (gal)	172670
Pumping time, t_e (min)	151.6
Net pressure (end time), p_{net} (psi)	169.4
Proppant conc. (end time), c_{add} (ppga)	9

TABLE 3.6−PUMPING SCHEDULE FOR CASE 2

	Start time (min)	End time (min)	c_{add} (ppga)	Proppant used (lbm)	Liquid used (gal)
Pad	0	68	0	0	86020
1	68	71	1	2920	2920
2	71	75	2	10550	5280
3	75	82	3	24610	8200
4	82	91	4	37840	9460
5	91	102	5	58020	11600
6	102	113	6	72130	12020
7	113	127	7	94890	13560
8	127	141	8	107160	13400
9	141	151	9	91870	10210

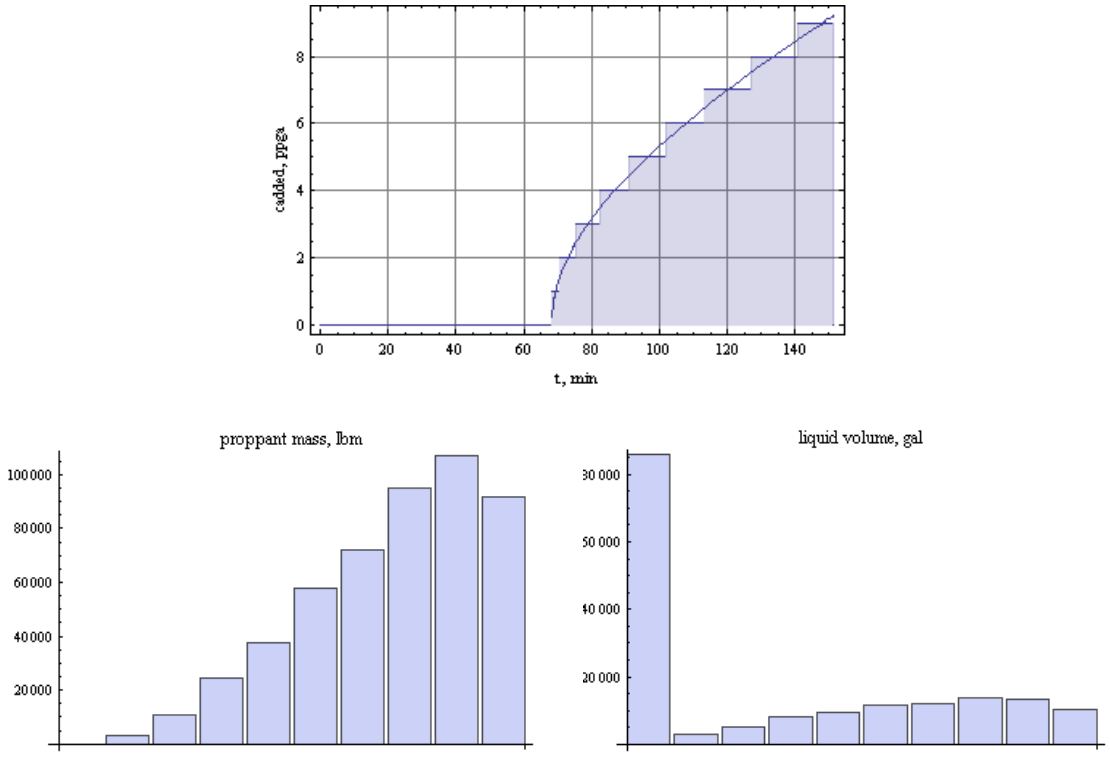

Fig. 3.5−(top) Proppant concentration schedule, (bottom left) amounts of proppants required for each stage, (bottom right) liquid volume used for each stage for case 2

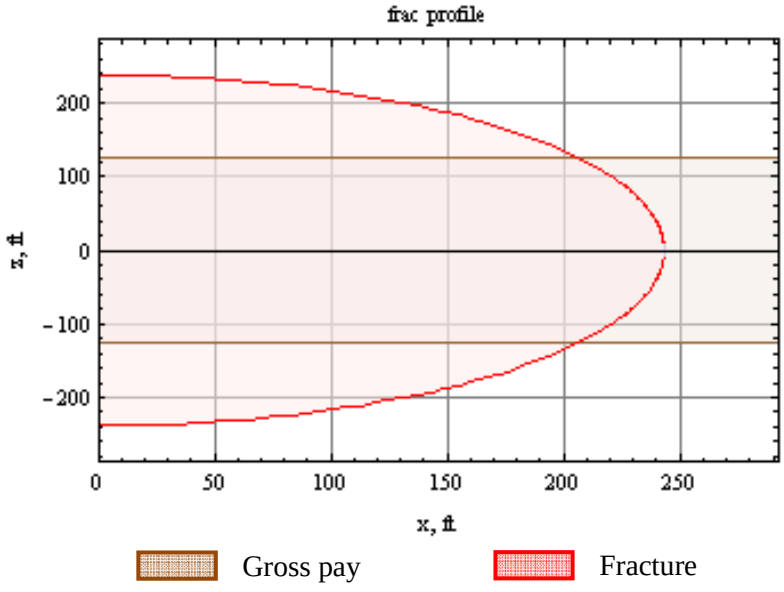

Fig. 3.6−Fracture geometry at the end of the job for case 2

Case 3: $\Delta\sigma_u$ = 300 psi and $\Delta\sigma_d$ = 150 psi

In this example, the stress differences of the target layer and upper and lower bounding formation ($\Delta\boldsymbol{\sigma_u}$, $\Delta\boldsymbol{\sigma_d}$) are 300 and 150 psi, respectively. The final solution of fracture height for this case is out of the valid range of both original and simplified equilibrium height. As a result, the solution of this case is determined based on the assumption that the net pressure at the end of the job equals to the average stress difference of the reservoir and adjacent layers ($\boldsymbol{p_{net}} = \Delta\boldsymbol{\sigma}$). In this case, the average stress difference is 225 psi and the calculated fracture height is 349.4 ft.

The fracture dimensions and important parameters for hydraulic fracturing operation are shown in **Table 3.7**. The proppant concentration schedule, required proppant and clean liquid for each step of pumping are shown in **Table 3.8** and **Fig. 3.7**. Fracture geometry at the end of the job is illustrated as **Fig. 3.8**.

TABLE 3.7− SUMMARY OF CALCULATED FRACTURE DIMENSIONS AND PARAMETERS FOR FRACTURE OPERATION FOR CASE 3

Fracture Dimensions	
Frac height, h_f (ft)	349.4
Frac half-length, x_f (ft)	267.3
Frac ave width, w_{ave} (in)	0.28
Hydraulic Fracturing Parameters	
Number of proppant, N_{prop}	0.28324
Dimensionless productivity index, J_D	0.612
Dimensionless fracture conductivity, FcD	1.727
Penetration ratio, I_x	0.4050
Slurry efficiency, η (%)	37.39
Prop. mass, M_{prop} (lbm)	500000
Clean fluid vol. (gal)	133843
Pumping time, t_e (min)	120.5
Net pressure (end time), p_{net} (psi)	225.0
Proppant conc. (end time), c_{add} (ppga)	12

TABLE 3.8−PUMPING SCHEDULE FOR CASE 3

	Start time (min)	End time (min)	c_{add} (ppga)	Proppant used (lbm)	Liquid used (gal)
Pad	0	55	0	0	69190
1	55	56	1	1420	1420
2	56	58	2	4950	2470
3	58	62	3	11580	3860
4	62	66	4	17480	4370
5	66	71	5	26950	5390
6	71	76	6	33040	5510
7	76	82	7	43740	6250
8	82	88	8	48810	6100
9	88	95	9	59870	6650
10	95.41	102.26	10	63340	6330
11	102.26	109.76	11	74330	6760
12	109.76	120.63	12	114490	9540

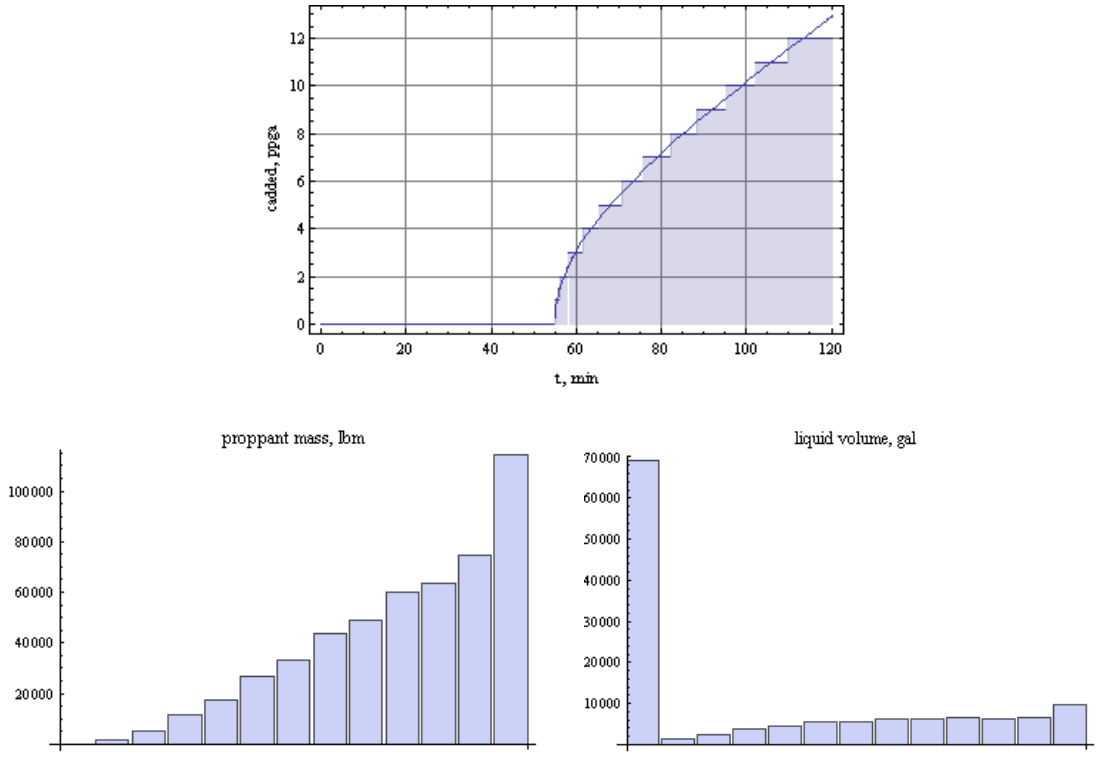

Fig. 3.7−(top) Proppant concentration schedule, (bottom left) amounts of proppants required for each stage, (bottom right) liquid volume used for each stage for case 3

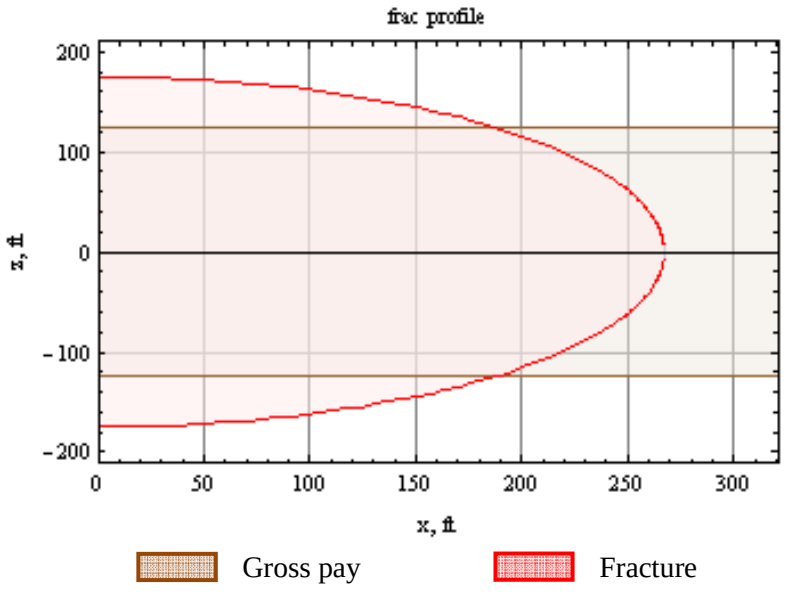

Fig. 3.8−Fracture geometry at the end of the job for case 3

Case 4: $\Delta\sigma_u$ = 150 psi and $\Delta\sigma_d$ = 150 psi

In this example, the stress differences of the target layer and upper and lower bounding formation ($\Delta\boldsymbol{\sigma_u}$, $\Delta\boldsymbol{\sigma_d}$) are 300 and 150 psi, respectively. The final solution of fracture height for this case is out of the valid range of both original and simplified equilibrium height. The fracture height which is calculated based on the assumption that ***pnet*** = $\Delta\boldsymbol{\sigma}$ gives the fracture aspect ratio less than 1. This result conflicts to the assumption used to derive PKN model where the fracture length is approximately greater than the fracture height. As a result, the solution of this case is determined based on the assumption that the aspect ratio is equal to 1.

The fracture dimensions and important parameters for hydraulic fracturing operation are shown in **Table 3.9**. The proppant concentration schedule, required proppant and clean liquid for each step of pumping are shown in **Table 3.10** and **Fig. 3.9**. Fracture geometry at the end of the job is illustrated as **Fig. 3.10**.

TABLE 3.9−SUMMARY OF CALCULATED FRACTURE DIMENSIONS AND PARAMETERS FOR FRACTURE OPERATION FOR CASE 4

Fracture Dimensions	
Frac height, h_f (ft)	483.9
Frac half-length, x_f (ft)	242.0
Frac ave width, w_{ave} (in)	0.24
Hydraulic Fracturing Parameters	
Number of proppant, N_{prop}	0.22627
Dimensionless productivity index, J_D	0.575
Dimensionless fracture conductivity, FcD	1.683
Penetration ratio, I_x	0.3666
Slurry efficiency, η (%)	37.93
Prop. mass, M_{prop} (lbm)	500000
Clean fluid vol. (gal)	174543
Pumping time, t_e (min)	153.1
Net pressure (end time), p_{net} (psi)	167.0
Proppant conc. (end time), c_{add} (ppga)	9

TABLE 3.10−PUMPING SCHEDULE FOR CASE 4

	Start time (min)	End time (min)	c_{add} (ppga)	Proppant used (lbm)	Liquid used (gal)
Pad	0	69	0	0	86820
1	69	71	1	3020	3020
2	71	76	2	10910	5460
3	76	84	3	25440	8480
4	84	92	4	39170	9790
5	92	104	5	60040	12010
6	104	116	6	74690	12450
7	116	130	7	98230	14030
8	130	144	8	111010	13880
9	144	153	9	77480	8610

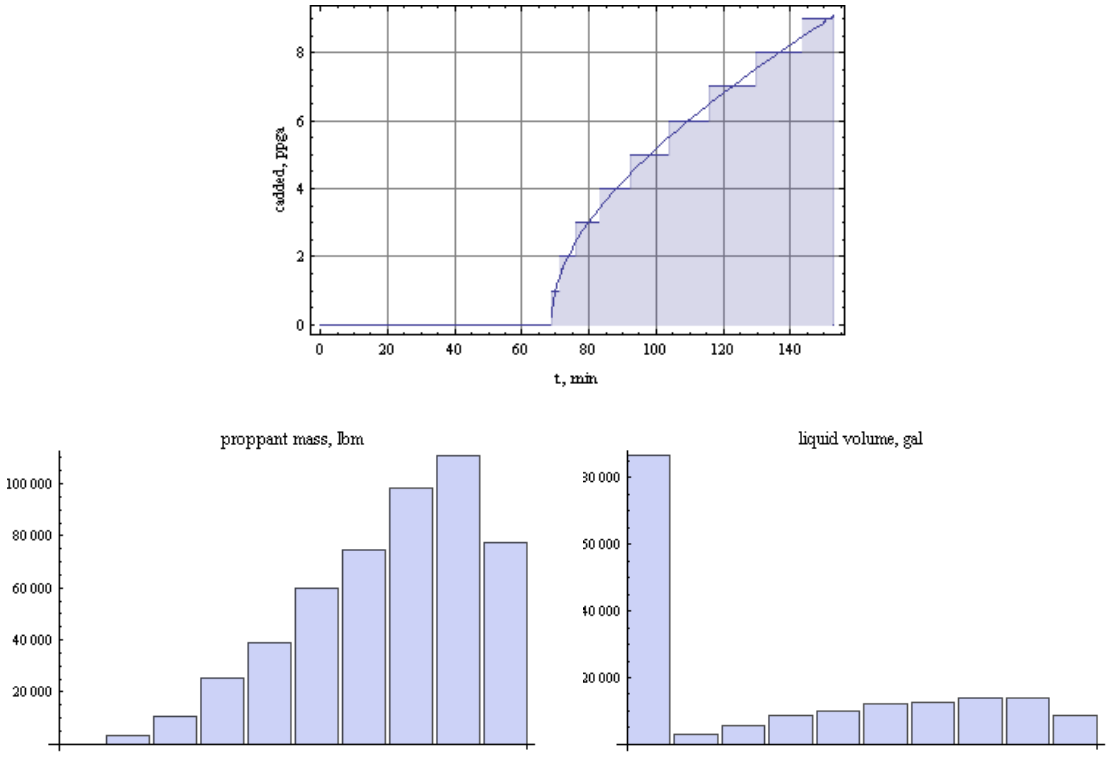

Fig. 3.9−(top) Proppant concentration schedule, (bottom left) amounts of proppants required for each stage, (bottom right) liquid volume used for each stage for case 4

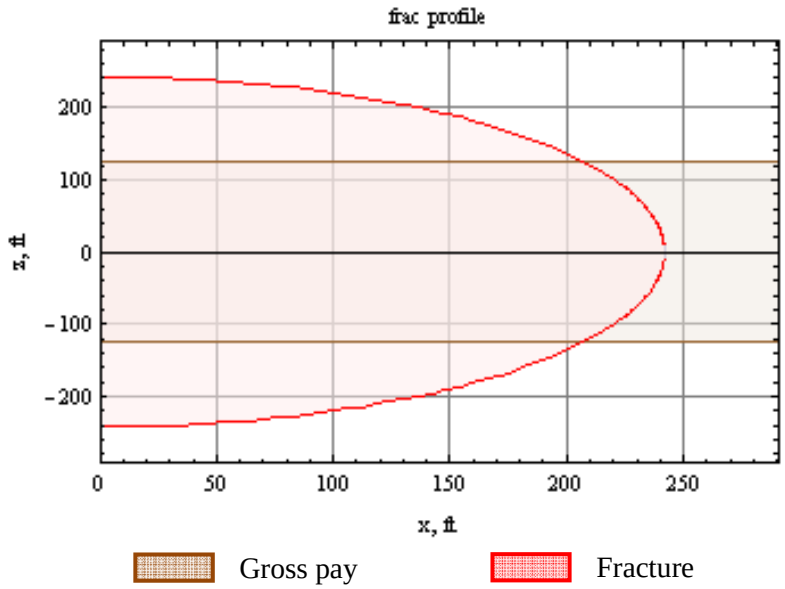

Fig. 3.10−Fracture geometry at the end of the job for case 4

However, not only the stress differences but also any other input parameters affect the calculation procedures or criterions of calculation as shown in the next example.

Case 5: $\Delta\sigma_u$ = 500 psi, $\Delta\sigma_d$ = 500 psi and E' = 2.0×10^6 psi

In this example, reservoir, proppant, fracture fluid and rock properties including the stress differences are the same as used for the first case except that the plane strain modulus changes from 1.5×10^6 psi to 2.0×10^6 psi. With the same stress differences, the valid range of original equilibrium height is the same as well. However, changing in the plane strain modulus causes shifting up the net pressure line obtained from the fracture design which is represented by the pink line in **Fig. 3.11**. From the figure, the final solution cannot be obtained in the valid range. As a result, the simplified version of equilibrium height is applied to determine the fracture height. It is approximately 394.8 ft.

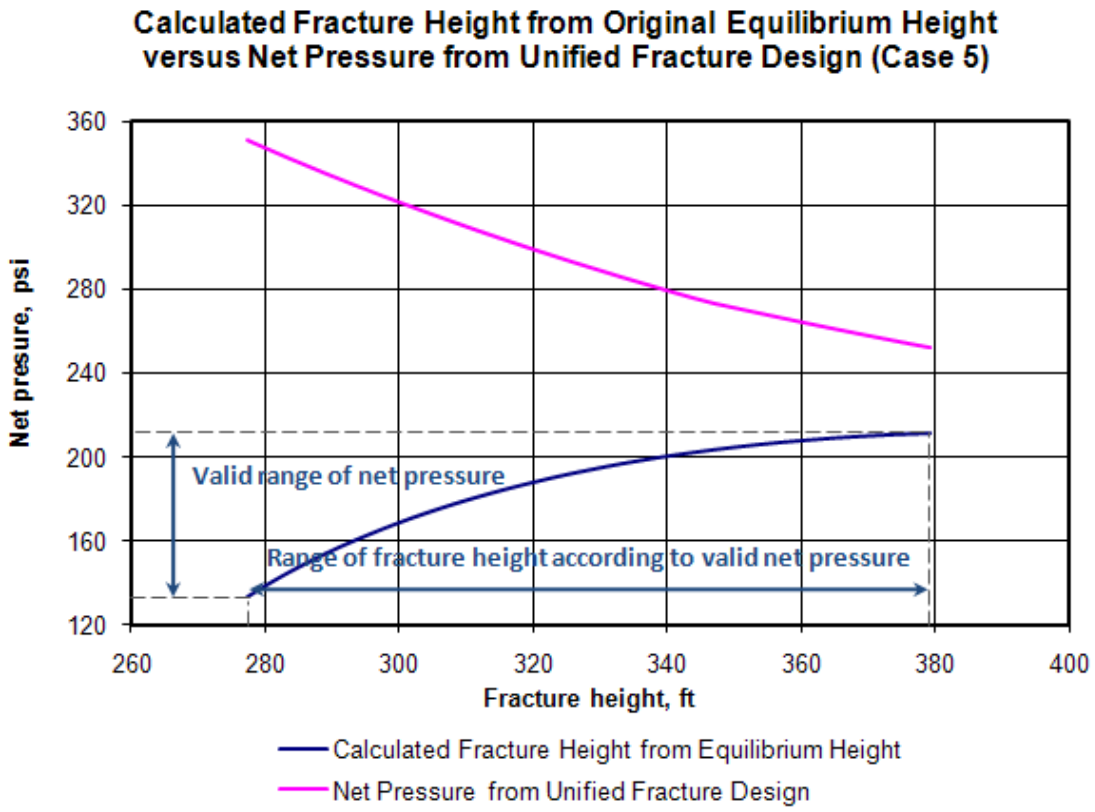

Fig. 3.11−The plot of calculated fracture height using original equilibrium height concept (blue line) versus net pressure from fracture design (pink line) for case 5. The final solution (the intersection) is out of the valid range of calculation

The fracture dimensions and important parameters for hydraulic fracturing operation are shown in **Table 3.11**. The proppant concentration schedule, required proppant and clean liquid for each step of pumping are shown in **Table 3.12** and **Fig. 3.12**. Fracture geometry at the end of the job is illustrated as **Fig. 3.13**.

TABLE 3.11− SUMMARY OF CALCULATED FRACTURE DIMENSIONS AND PARAMETERS FOR FRACTURE OPERATION FOR CASE 5

Fracture Dimensions	
Frac height, h_f (ft)	394.8
Frac half-length, x_f (ft)	258.7
Frac ave width, w_{ave} (in)	0.27
Hydraulic Fracturing Parameters	
Number of proppant, N_{prop}	0.26295
Dimensionless productivity index, J_D	0.599
Dimensionless fracture conductivity, FcD	1.711
Penetration ratio, I_x	0.3920
Slurry efficiency, η (%)	35.85
Prop. mass, M_{prop} (lbm)	500000
Clean fluid vol. (gal)	140713
Pumping time, t_e (min)	126.0
Net pressure (end time), p_{net} (psi)	243.3
Proppant conc. (end time), c_{add} (ppga)	12

TABLE 3.12−PUMPING SCHEDULE FOR CASE 5

	Start time (min)	End time (min)	c_{add} (ppga)	Proppant used (lbm)	Liquid used (gal)
Pad	0	59	0	0	74940
1	59	61	1	1700	1700
2	61	63	2	5350	2670
3	63	67	3	12700	4230
4	67	71	4	18110	4530
5	71	76	5	28490	5700
6	76	82	6	33400	5570
7	82	88	7	45240	6460
8	88	94	8	48510	6060
9	94	102	9	60980	6780
10	101.5	108.22	10	62140	6210
11	108.22	115.78	11	74880	6810
12	115.78	126.09	12	108490	9040

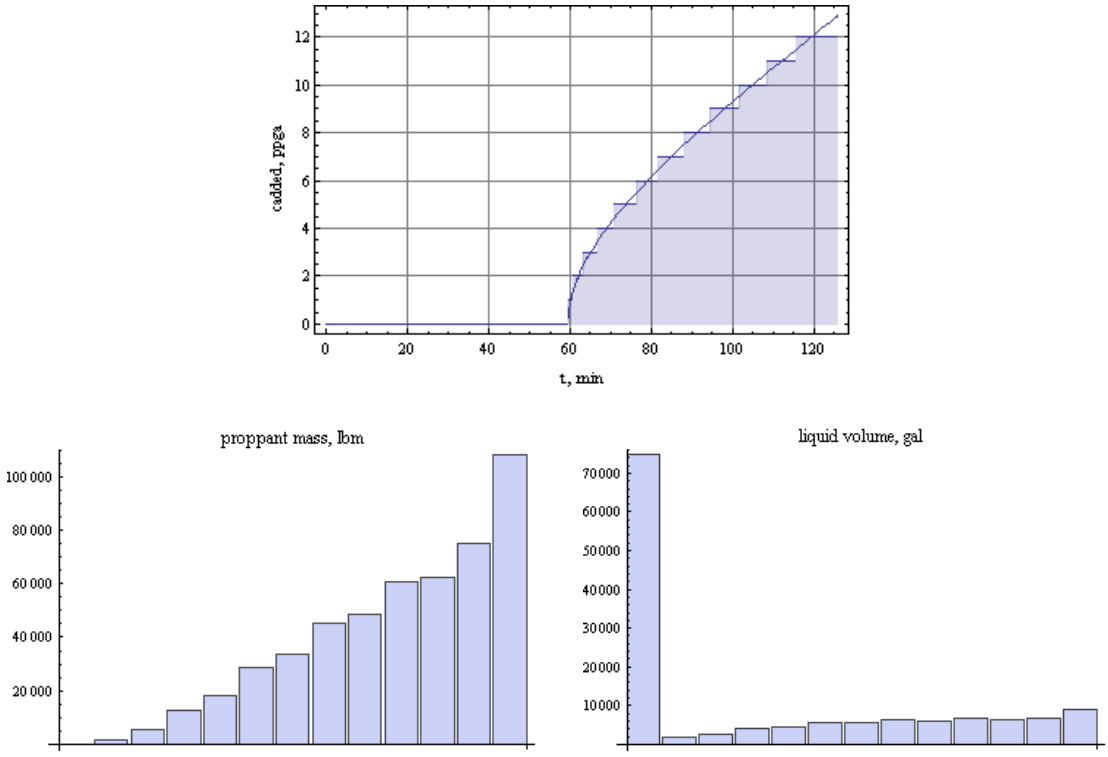

Fig. 3.12−(top) Proppant concentration schedule, (bottom left) amounts of proppants required for each stage, (bottom right) liquid volume used for each stage for case 5

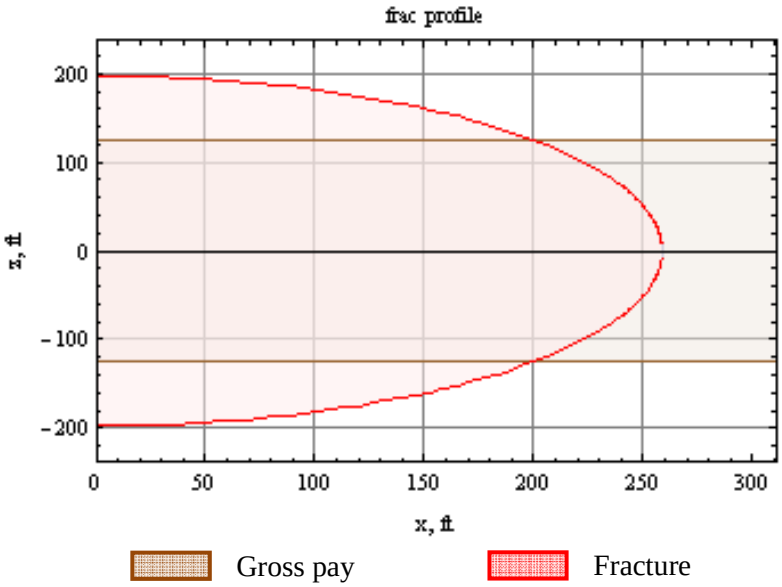

Fig. 3.13−Fracture geometry at the end of the job for case 5

3.2 Comparison between Theoretical Fracture Dimensions from Modified Unified Fracture Design and Estimate of Fracture Geometry from FRACCADE

FRACCADE is a commercial fracture design program. It was developed by Schlumberger. The concept of FRACCADE is to determine the pumping schedules to achieve the fracture that has the desired fracture half-length. As a result, the desired fracture half-length is required as an initial guess for the iterative calculation. In addition, it can estimate fracture geometry at the end of the job. FRACCADE offers both of 2D (PKN, KGN and radial) and 3D (pseudo 3D) model to determine fracture geometry.

In this section, two sets of field data were used to evaluate the theoretical fracture dimensions providing the maximum productivity index based on the given amount of proppants using our program (incorporating rigorous height determination into the unified fracture design). Then, the estimate of actual fracture geometry after fracturing was determined using FRACCADE associated with treatment schedules based on calculated fracture dimensions and compared to the theoretical results from our program.

Well-A

The objective is to create a fracture in a clean sandstone layer. The reservoir has 60 acres of drainage area. Thickness of net pay and gross pay are the same and equal to 13.8 ft. Permeability of the reservoir is 150 md. The target layer has 4047 psi of closure stress and 0.59×10^{6} psi of plane strain modulus. Upper and lower bounding layers have

4143 psi and 4162 psi of closure stress, respectively. Fracture toughness of both bounding layers is 1000 psi-in$^{0.5}$. The amount of proppants available for this job is 17500 lbm. Proppant specific gravity is 2.7. Proppant packed porosity with and without stress are 0.35 and 0.38, respectively. Fracture permeability is 216340 md. Injection rate of slurry is 15 bpm (two wings). The rheology properties of fracture fluid are 0.59 of flow behavior index and 0.0534 of consistency index. It is assumed that leak-off coefficient of net pay is 0.0023 ft/min$^{0.5}$, spurt loss is negligible and fluid loss of bounding layers is half of that of pay zone. The input parameters of this example can be summarized as shown in **Table 3.13**.

According to the input data, the theoretical fracture dimensions providing the maximum productivity index based on the given mass of proppants were computed using our program. The fracture dimensions and important parameters for hydraulic fracturing operation are shown in the second column of **Table 3.14.** Then, the estimate fracture geometry after fracturing was obtained from FRACCADE based on the calculated fracture half-length from our program as an initial guess. For the first run (the third column of **Table 3.14)**, radial model without tip-screen out was used for fracture geometry estimation. It can be observed that the fracture geometry after fracturing is a little bit different from the theoretical one. For the second run (the last column of **Table 3.14)**, the radial model with tip-screen out was tried to obtain the fracture geometry which is more identical to the theoretical one. However, it requires more mass of proppant to be pumped for tip-screen out because it is necessary to increase the proppant

concentration at the end (tip) of fracture to restrict the fracture growth in propagating direction.

TABLE 3.13−SUMMARY OF INPUT PARAMETERS OF WELL-A

Reservoir info.	
Permeability	150.0 md
Drainage area	60 acre
Net pay thickness	13.8 ft
Gross pay thickness (perforated interval)	13.8 ft
Rock properties	
Plane strain modulus	0.59×10^6 psi
K_{IC}	1000 psi-$in^{0.5}$
Closure stress of reservoir (σ_{mid})	4047 psi
Closure stress of upper bounding layer (σ_{top})	4143 psi
Closure stress of lower bounding layer (σ_{bot})	4162 psi
Proppants properties	
Total proppant mass	16,600 lbm
Proppant retained permeability	216,340 md
Specific gravity	2.7
Proppant pack porosity	0.38
Proppant pack porosity under closure stress	0.35
Fluid properties	
Rheology flow behavior index, n	0.59
Rheology consistency index, K	0.0534 lbf $\times s^n$ / ft^2
Slurry rate	15 bpm
Leakoff coefficient in net pay	0.0023 ft/$min^{0.5}$
Spurt loss	neglect
Fluid loss multiplier out of net pay	0.5

TABLE 3.14−COMPARISON OF FRACTURE DIMENSIONS AND OTHER PARAMETERS FROM OUR PROGRAM AND FRACCADE FOR WELL-A

	Modified Unified Fracture Design	FRACCADE (1)	FRACCADE (2)
Model/Assumption for fracture geometry determination	Equilibrium Height	Radial model without TSO	Radial model with TSO
Initial guess of half-length		36.1	50.0
Net pay, h_{np} (ft)	13.8	13.8	13.8
Permeability, k (md)	150.0	150.0	150.0
Frac height, h_f (ft)	86.6	98.1	84.8
Frac half length, x_f (ft)	36.1	43.6 ($x_{f,opt}$ = 33.0)*	36.8 ($x_{f,opt}$ = 72.3)*
Frac ave width, w_{ave} (in)	0.49	0.19 ($w_{ave,opt}$ = 0.45)*	1.10 ($w_{ave,opt}$ = 0.98)*
Number of proppant, N_{prop}	0.00327	0.00273	0.01309
Dimensionless productivity index, J_D	0.26	0.251 ($J_{D,opt}$ = 0.253)*	0.297 ($J_{D,opt}$ = 0.317)*
Dimensionless fracture conductivity, C_{fD}	1.636	0.938 ($C_{fD,opt}$ = 1.636)*	6.318 ($C_{fD,opt}$ = 1.636)*
Penetration ratio, I_x	0.0447	0.054 ($I_{x,opt}$ = 0.040)*	0.046 ($I_{x,opt}$ = 0.089)*
Prop. mass, M_{prop} (lbm)	17500	16500	68600
Proppant conc. (end time), c_{add} (ppga)	34.643	31.973	55.8975

* Optimum values of each parameters based on proppant mass and fracture height obtained from FRACCADE

Well-B

The objective is to create a fracture in multilayer sandstone using tip screen-out technique. Each layer has different rock properties. Rock properties of each layer are shown in **Table 3.15**.

TABLE 3.15−ROCK PROPERTIES OF EACH LAYER OF WELL-B

Formation	Gross Height (ft)	Net Height (ft)	Closure Strees (psi)	Permeability (md)	Plane Strain Modulus (psi)
SHALE	56.8	0	16287	1.5	1.54E+06
Dirty Sandstone	49.8	35	16198	143.6	9.49E+05
SHALE	72.6	0	16514	0.1	1.97E+06
Clean Sandstone	**80**	**76**	**15999**	**696.6**	**5.91E+05**
SHALE	22.2	11	16034	3.3	1.43E+06
Dirty Sandstone	12.9	9	16048	21.3	1.18E+06
SHALE	5.8	3	16056	23.2	1.15E+06
Clean Sandstone	8	7	16062	449.0	6.62E+05
SHALE	7.4	4	16068	0.7	1.31E+06
Clean Sandstone	13.9	12	16076	2055.8	3.95E+05
SHALE	123.5	0	16707	39.8	1.54E+06
Total	272.6	157.0			
Average			16068		9.59E+05

The reservoir has 60 acres of drainage area. Total thickness of net pay and gross pay of the reservoir are 157.0 ft and 272.6 ft, respectively. It is assumed that the layer which has the smallest minimum in-situ stress represents the target layer because fracture tends to be first initiated in this formation. As a result, closure stress and strain modulus used for computing fracture design is 15999 psi and 0.591×10^{6} psi of plane. Weighted average is applied to determine the average permeability which is equal to 548.3 md.

Top and bottom bounding formations have 16287 psi and 16707 psi of closure stress, respectively. Fracture toughness of both bounding layers is 1000 psi-$in^{0.5}$. The amount of proppants available for this job is 220000 lbm. Proppant specific gravity is 2.65 . Proppant packed porosity with and without stress are 0.35 and 0.38, respectively. Fracture permeability is 110000 md. Injection rate of slurry is 35 bpm (two wings). The rheology properties of fracture fluid are 0.33 of flow behavior index and 0.291 of

consistency index. It is assumed that leak-off coefficient of net pay is 0.002 ft/min$^{0.5}$, spurt loss is negligible and fluid loss of bounding layers is half of that of pay zone. The input parameters of this example can be summarized as shown in **Table 3.16**.

TABLE 3.16−SUMMARY OF INPUT PARAMETERS OF WELL-B

Reservoir info.	**Case 1**
Permeability	548.3 md
Drainage area	60 acre
Net pay thickness	157 ft
Gross pay thickness (perforated interval)	272.6 ft
Rock properties	
Plane strain modulus	0.591 ×106 psi
K_{IC}	1000 psi-in0.5
Closure stress of reservoir (σ_{mid})	15999 psi
Closure stress of upper bounding layer (σ_{top})	16287 psi
Closure stress of lower bounding layer (σ_{bot})	16707 psi
Proppants properties	
Total proppant mass	215,500 lbm
Proppant retained permeability	110,000 md
Specific gravity	2.65
Proppant pack porosity	0.38
Proppant pack porosity under closure stress	0.35
Fluid properties	
Rheology flow behavior index, n	0.33
Rheology consistency index, K	0.291 lbf ×sn / ft2
Slurry rate	35 bpm
Leakoff coefficient in net pay	0.002 ft/min0.5
Spurt loss	neglect
Fluid loss multiplier out of net pay	0.5

Assuming that the fracture would cover the whole gross pay (8 sub-layers), the theoretical fracture dimensions providing the maximum productivity index based on the given mass of proppants were computed using our program. The fracture dimensions and important parameters for hydraulic fracturing operation are shown in the second column of **Table 3.17.** Then, the estimate fracture geometry after fracturing was obtained from FRACCADE based on the calculated fracture half-length from our program as an initial guess using Pseudo 3D model as shown in the third column of **Table 3.17**. It was found that the fracture could cover only 7 sub-layers of the reservoir. As a result, the first design from our program was not reliable because of fault assumption. As a result, the redesign from our program was attempted by assuming that the fracture covers only 7 sub-layers. As a result, the net pay, gross pay and average permeability used for the redesign changed to 122 ft, 150.2 ft and 664.4 md, respectively. Shale layer on top of the sub-layer which has the smallest minimum in-situ stress is considered as new upper bounding layer. Its closure stress is 16514 psi. The fracture dimensions and important parameters for hydraulic fracturing operation of the redesign are shown in the last column of **Table 3.17.**

TABLE 3.17−COMPARISON OF FRACTURE DIMENSIONS AND OTHER PARAMETERS FROM OUR PROGRAM AND FRACCADE FOR WELL-B

	Modified Unified Fracture Design (1)	FRACCADE	Modified Unified Fracture Design (2)
Model/Assumption for fracture geometry determination	Equilibrium Height	Pseudo 3D model with TSO	Equilibrium Height
Initial guess of half-length		25.4	
Net pay, h_{np} (ft)	157.0	122.0	122.0
Permeability, k (md)	548.3	664.4	664.4
Frac height, h_f (ft)	280.1	230.5	161.5
Frac half length, x_f (ft)	25.5	30.2 ($x_{f,opt}$ = 72.3)*	28.8
Frac ave width, w_{ave} (in)	2.49	1.31 ($w_{ave,opt}$ = 3.04)*	3.42
Number of proppant, N_{prop}	0.00162	0.00165	0.00208
Dimensionless productivity index, J_D	0.24	0.237 ($J_{D,opt}$ = 0.238)*	0.25
Dimensionless fracture conductivity, C_{fD}	1.636	1.181 ($C_{fD,opt}$ = 1.636)*	1.636
Penetration ratio, I_x	0.0315	0.0374 ($I_{x,opt}$ = 0.0317)*	0.0357
Prop. mass, M_{prop} (lbm)	220000	220000	220000
Proppant conc. (end time), c_{add} (ppga)	128.212	161.84	215.27

* Optimum values of each parameters based on proppant mass and fracture height obtained from FRACCADE

However, it can be observed that the fracture dimensions from our program and the estimate of actual fracture geometry after treatment from FRACCADE are so different. This is because 2D fracture propagation models used for calculation in the current version of modified unified fracture design are not sufficient to estimate fracture

geometry in multilayer reservoir. As a result, our program is deficient of handling multilayer (more than 3 layers) problem.

3.3 Discussions

According to the applications and results of all the cases study from add-in fracture design program and comparison between theoretical fracture dimensions from modified unified fracture design and estimate of fracture geometry from FRACCADE, many interesting points can be observed as shown in the followings:

i. The primary method of fracture height calculation of this study is referred to the equilibrium height. This method has a limitation of calculation where the valid range of net pressure which can be derived from the stress contrast between the reservoir and bounding formations is limited. As a result, in some cases that the stress contrast is too low or too high, fracture height cannot be computed by this method as shown in **Section 3.1** (see case 2, 3 and 4). In other words, this method is valid only limited values of stress differences or minimum in-situ stress distribution (reservoir and adjacent formations). **Fig. 3.14** demonstrates an effect of changing in stress differences on the valid range of net pressure for fracture height calculation (using information from case 1 and case 2 in **Section 3.1**).

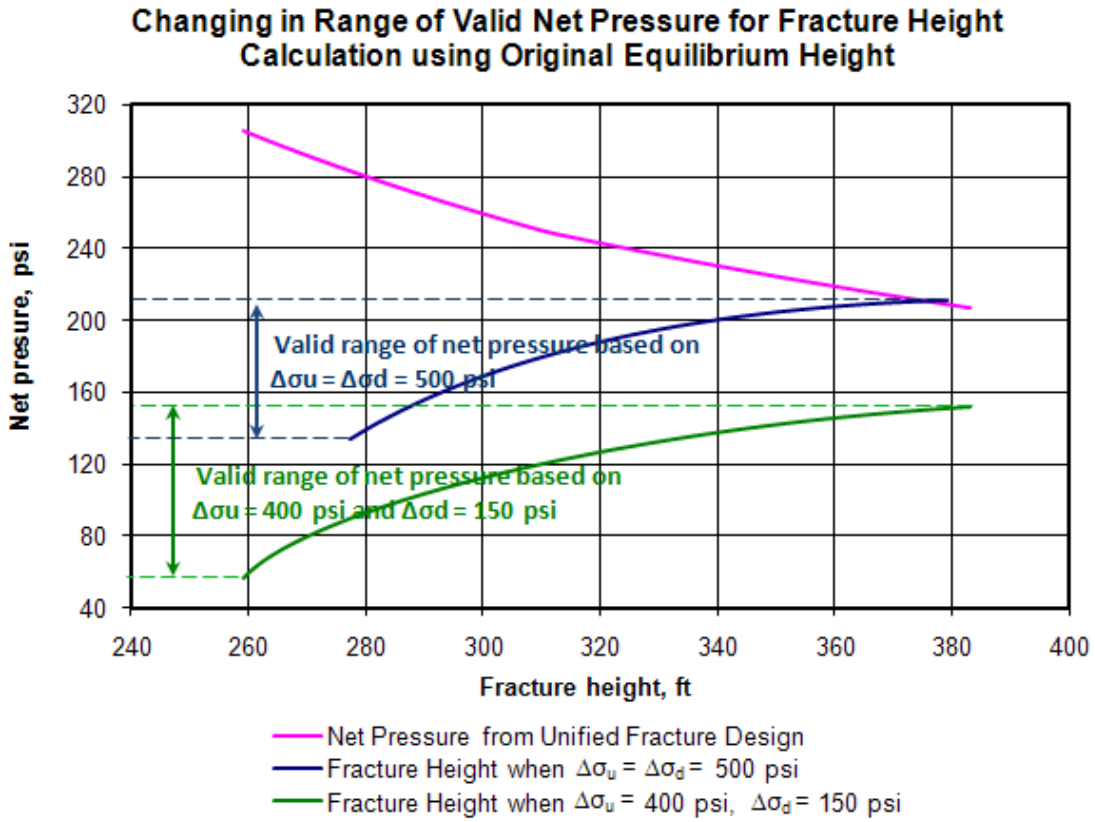

Fig. 3.14−The effect of changing in stress differences, $\Delta\sigma_u$ and $\Delta\sigma_d$, on valid range of net pressure for fracture height calculation

From the plot, decreasing in the stress differences causes lowering the value of valid net pressure (shifting down of the bottom line). As a result, the intersection or final solution is not in the valid range of the equilibrium height or the fracture height cannot be computed by this method. This is a significant limitation of the concept. Thus, some assumptions are required to make the program applicable to any cases.

ii. Not only stress differences or minimum in-situ stress distribution, but also other parameters related to hydraulic fracturing job; for example plane strain modulus, injection rate and fracture fluid properties, affect the calculation of fracture height. **Fig. 3.15** demonstrates an effect of changing in plane strain modulus on fracture height calculation. (using information from case 1 and case 5 in **Section 3.1**)

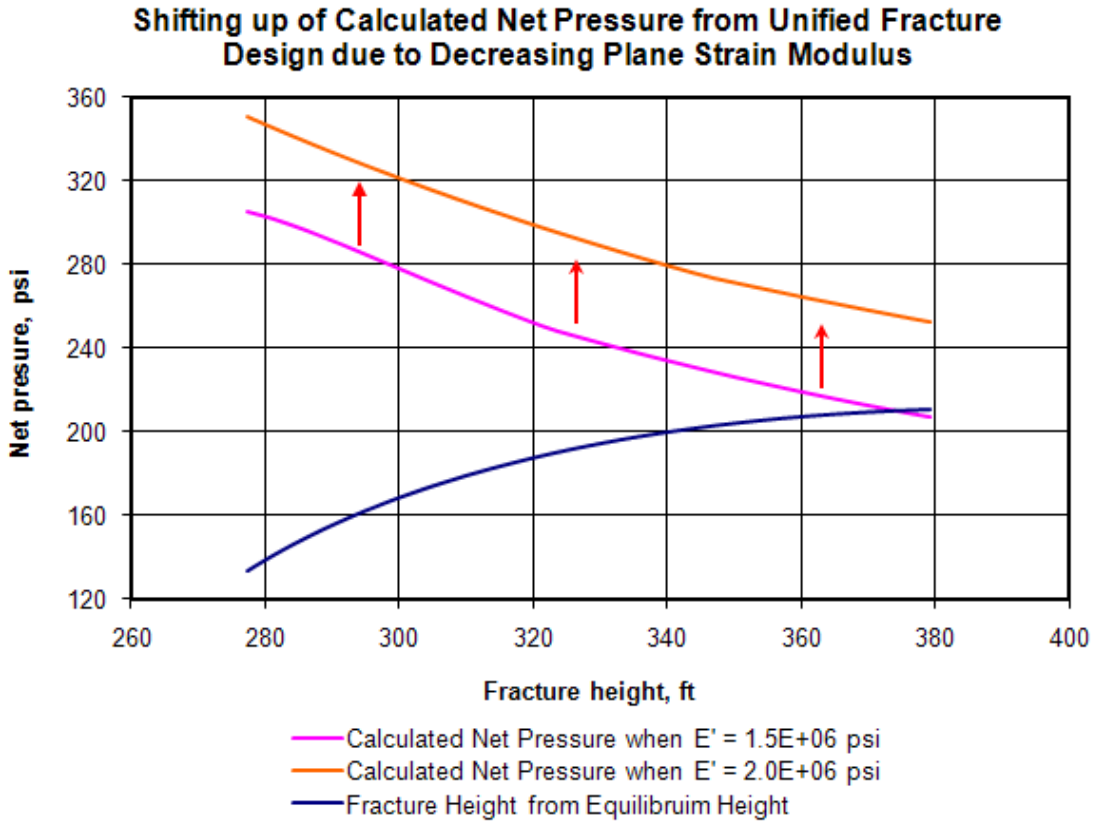

Fig. 3.15−The effect of changing in plane strain modulus, *E'*, on fracture height calculation

This can happen when fracturing engineers perform mini-frac job and obtain new information such as plane strain modulus of target formation, which is

different from which they used for the initial design. The new information is used for redesign. According to this example, the new plane strain modulus causes failure in fracture height calculation using the equilibrium height (shifting up of the top line). However, the effect of increasing in plane strain modulus can be compensated by adjusting other parameters; for example, reducing injection rate and changing type of fracture fluid. On the other hand, if other parameters remain the same, the fracture height must be calculated by other methods (different assumption).

iii. In some cases, the final solution of fracture height cannot be obtained from the original equilibrium height. This is because for the given condition (or input data), the calculated net pressure at both tips are too high or too low. As a result, it cannot satisfy the equilibrium height. For example, the calculated net pressure at the center of crack plus hydrostatic pressure overcomes the minimum in-situ stress of lower bounding layer. As a result, there is no limit of fracture growth downward that is unrealistic.

iv. Result obtained from the modified unified fracture design which is theoretical fracture dimensions providing the maximum productivity index is used to determine the treatment schedule and fracture geometry after treatment using FRACCADE. According to the results from well-A in **Section 3.1** (only the cases that the required amount of proppants from the design are similar), the

theoretical fracture dimensions from our program and the estimate of fracture geometry from FRACCADE using radial model without tip-screen out are a little bit different because, in our program, the fracture is assumed to have a perfect elliptical shape for PKN model or a uniform fracture width for KGD model. In other words, it does not take effect Young's modulus and Poisson's ratio of bounding layers into account for calculation. These two parameters used to derive plan strain modulus. Then, the plane strain modulus is used to calculate the hydraulic fracture width which affects net pressure calculation directly. The effect of non-uniformity of plane strain modulus of reservoir and bounding layers on the fracture width is shown in **Fig. 3.16**. Therefore, the fracture model used to determine fracture geometry in this program is needed further development to include the effect of Young's modulus and Poisson's ratio of bounding layers. This will help the program evaluate more accurate of fracture geometry and offer more realistic fracture design.

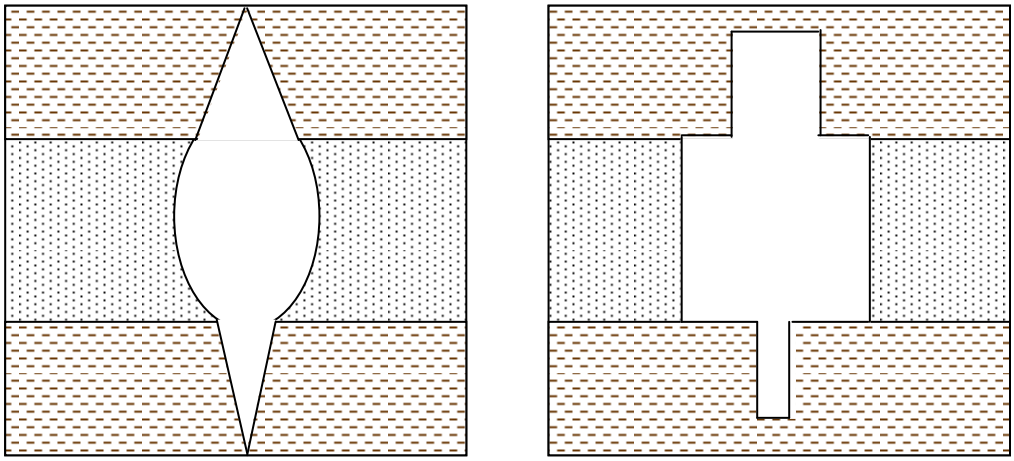

Fig. 3.16−(Left) Imperfect elliptical shape (PKN) and (Right) non-uniform fracture width (KGD) of fracture due to non-uniformity of plane strain modulus of reservoir and bounding layers

v. From case study of Well-B, the theoretical fracture dimensions from our program and the estimate of fracture geometry from FRACCADE are significantly different. As a result, it can be said that one of remarkable limitations of our program is deficiency of handling multilayer formation problem. It requires more complicated fracture model to solve this kind of problem. Full 3D and pseudo 3D (P3D) models should be appended to the program for solving the multilayer reservoir problem to obtain more realistic fracture design.

CHAPTER IV

CONCLUSIONS

4.1 Summary

The key of success to achieve the optimum reservoir performance after fracturing is the fracture design. The good design will give the fracture dimensions that would maximize the post-treatment productivity index. This fracture geometry can be estimated by means of the unified fracture design methodology.

The fracture height is a primary parameter for this technique. Thus, the accuracy of the fracture height estimation is very significant. Currently, unified fracture design does not provide a mechanism to estimate the fracture height. This research offers a reasonable approach to couple the fracture height estimation with the unified fracture design. We have shown that the program is applicable in a wide range of input data. For the single layer reservoirs, the theoretical fracture dimensions from our program are consistent with the estimates of fracture geometry using FRACCADE.

4.2 Recommendations

We have been successful estimating the fracture geometry for single layer reservoirs. However, because unified fracture design relies in a strictly 2D model for fracture propagation, the errors of the estimates of fracture dimensions for multilayer reservoirs can be high. As a result, the further development of the program is still needed. The 3D model should be appended to the program for improvement.

REFERENCES

Anderson, G.D. 1981. Effects of Friction on Hydraulic Fracture Growth near Unbounded Interfaces in Rocks. Paper SPE 8347-PA presented at the SPE Annual Technical Conference and Exhibition, Las Vegas, 23-26 September. DOI: 10.2118/8437-PA.

Barenblatt, G.I. 1962. The Mathematical Theory of Equilibrium Cracks in Brittle Fracture. *Advances in Applied Mechanics*, **7:** 55-129. DOI: 10.1016/S0065-2156(08)70121-2

Economides, M.J., Oligney, R., and Valko, P.P. 2002. *Unified Fracture Design: Bridging the Gap between Theory and Practice*. Orsa Press, Alvin Texas: 23-129.

Hubbert, M.K., and Willis, D.G. 1957. Mechanics of Hydraulic Fracturing. *Trans. AIME* **210:** 153-166.

Irwin, G.R. 1957. Analysis of Stresses and Strains near the End of a Crack Traversing a Plate. *Journal of Applied Mechanics* **24:** 361-364.

Nolte, K.G. 1986. Determination of Proppant and Fluid Schedules from Fracturing Pressure Decline. Paper SPE 13278-PA presented at the SPE Annual Technical Conference and Exhibition, Houston, 16-19 September. DOI: 10.2118/13278-PA.

Perkins, T.K., and Kern, L.R. 1961. Width of Hydraulic Fractures. *Journal of Petroleum Technology* **13:** 937-949.

Rice, J.R. 1968. Fracture: An Advanced of Treatise. *Mathematical Analysis in the Mechanics of Fracture.* ed. H. Liewbowitz, 191-311. New York: Academic Press.

Simonson, E.R., Abou-Sayed, A.S. and Clifton, R.J. 1978. Containment of Massive Hydraulic Fractures. Paper SPE 6089-PA presented at the SPE Annual Technical Conference and Exhibition, New Orleans, 3-6 September. DOI: 10.2118/6089-PA.

Teufel, L.W. and Clark, J.A. 1984. Hydraulic Fracture Propagation in Layered Rock: Experimental Studies of Fracture Containment. Paper SPE 9878-PA presented at the SPE Annual Technical Conference and Exhibition, Denver, 27-29 May. DOI: 10.2118/9878-PA.

VITA

Name:	Termpan Pitakbunkate
Address:	Texas A&M University Petroleum Engineering Department 3116 TAMU 501 RICH College Station, Texas 77843-3116 Phone: 1-979-255-3845
Email Address:	termpanpitak@neo.tamu.edu
Education:	B.Eng. Petroleum Engineering, Chulalongkorn University, 2004 Bangkok, Thailand M.S. Petroleum Engineering, Texas A&M University, 2010 Texas, USA
Employment History:	PTT Exploration and Production, Thailand, 2004-2008

This thesis was typed by the author.